AZƏRBAYCAN MİLLİ ELMLƏR AKADEMİYASI

AZƏRBAYCAN ASTRONOMİYA JURNALI

2018, Cild 13, № 2

AZERBAIJAN NATIONAL ACADEMY OF SCIENCES

ASTRONOMICAL JOURNAL OF AZERBAIJAN

2018, Vol. 13, № 2

Bakı-2018 / Baku-2018

ASTRONOMICAL JOURNAL OF AZERBAIJAN

Founded in 2006 by the Azerbaijan National Academy of Sciences (ANAS)
Published in the Shamakhy Astrophysical Observatory (ShAO) named after N. Tusi, ANAS
ISSN: 2078-4163 (Print), 2078-4171 (Online)

Editorial board

Editorial Office address:	ANAS, 30, Istiglaliyyat Street, Baku, AZ-1001, the Republic of Azerbaijan
Address for letters:	ShAO, P.O.Box №153, Central Post Office, Baku, AZ-1000, Azerbaijan
E-mail:	aaj@shao.az
Phone:	(+994 12) 510 82 91
Fax:	(+994 12) 497 52 68
Online version:	http://www.aaj.shao.az

ASTRONOMICAL JOURNAL OF AZERBAIJAN

2018, Vol. 13, № 2

Contents

DETERMINATION OF THE ABUNDANCE OF "METALLICITY", CARBON AND SODIUM IN THE ATMOSPHERE OF STAR HR 7847 (F5IAB)

Z. A. Samedov [a,b*], ***A. M. Khalilov*** [a], ***A. R. Hasanova*** [a],

U. R. Gadirova [a], ***G. M. Hajiyeva*** [a], ***N. H. Samedova*** [a]

[a] *Shamakhy Astrophysical Observatory named after N.Tusi, Azerbaijan National Academy of Sciences, Shamakhy region, Azerbaijan*

[b] *Baku State University, Baku,Azerbaijan*

Spectrum of the star HR 7847(F5Iab) has been investigated on the basis of Coude spectrograms with dispersion of 8 Åmm and spectral resolution of 0.3 Å obtained at the 2 m telescope of the Shamakhy Astrophysical Observatory. On the FeII lines we have analyzed microturbulent velocity in the atmosphere of the star. It is defined ξ_t=5.0 km s^{-1}. The abundance of iron, carbon and sodium in the atmosphere of star HR7847 has been determined. It has been discovered that, in comparison with the solar chemical composition the abundance of carbon is less and the abundance of sodium is more. However, the abundance of iron is close to the abundance in the Sun.

Keywords: Supergiant – Fundamental parameters – Chemical composition

1. INTRODUCTION

Chemical composition is one of the most important parameters of stars. The advanced method to determine the chemical composition of the stars is the model method. This method is based on the construction of stars atmospheric models. Effective temperature and gravitational accelerationare basis parameters of atmosphere models, and stars evolutionary parameters - like their masses, radiuses, luminosity and ages can be determined by studying these parameters.

Study of microturbulence is important in order to determine the abundance of elements. This is because, equivalent width of the spectral lines depends on the microturbulence velocity and the abundance of elements is determined on the

* E-mail: zahir.01@mail.ru

basis of equivalent width of spectral lines. Microturbulence still does not have a generally accepted theory. That's why study of microturbulence is very important to understand the nature of this phenomenon.

According to modern evolutionary theory, as substances in A, F, G spectral type supergiant stars completely combine in a mixture process, outputs of CNO-cycle reach layers of the atmosphere of these stars. Consequently, in the atmosphere of these stars major alterations can occur in the initial abundance of C, N and O elements. According to modern evolutionary theory, in the atmosphere of A, F, G spectral type supergiant stars scarcity of carbon (C), nitrogen excess (N) and slight shortage of oxygen (O) must be observed.

Therefore according to modern evolutionary theory, study of chemical composition of the atmosphere of supergiant stars is one of the most pressing issues of astrophysics.

Boyarchuk and Lyubimkov [1] have discovered that, apart from discrepancy in the abundance sof C, N and O elements, excess of Na abundance can also be observed in the atmosphere of A, F, G spectral-type supergiant stars. It is considered that, excess of sodium abundance can be explained due to conversion of small amount of neons into sodium as the result of reactions in the NeNa cycle. As substances in A, F, G spectral type supergiant stars completely combine in a mixture process, sodiumis to be ousted to the atmosphere of these stars, and the abundance of sodium in the atmosphere should be changed. Thereby, determination of the abundance of sodium (Na) in the atmosphere of A, F, G spectral type supergiant stars is important from the standpoint of Galactic Chemical Evolution theory.

For this purpose, the atmosphere of the star HR7847(F5Iab) was determined. Microturbulent velocity, abundance of iron, carbon and sodium in the atmosphere of the star has been defined.

Observation materials were obtained on the basis of Coude spectrograms with dispersion of 8 Å/mm at the 2 m telescope of the Shamakhy Astrophysical Observatory and covers $\lambda\lambda$3700-5000 ÅÅ spectral region. W- equivalent width of spectral lines was measured. Equivalent width measurement error is no more than 7%. Equivalent width of $H\gamma$ line was measured as $W(H\gamma)$=5.643Å. Equivalent widths of NaI, CI and FeII lines are indicated in Table1.

2. MICROTURBULENT VELOCITY, ABUNDANCE OF ELEMENTS

In order to determine the microturbulent velocity ξ_t, atoms or ions of any element should have numerous lines covering large equivalent width Wλ diapason. Microturbulent velocity ξ_t is chosen in a such way that, the abundance of an element determined according to different lines does not change with the increase

of equivalent width Wλ. The most common lines on the spectrum of a star that we are studing are FeI lines and then FeII lines. But there is a significant impact to neutral iron lines from the discrepancies in LTE. If calculations are conducted on LTE position, the abundance determined according to FeI lines is less than the one (abundance) determined while refusing (suspending, waiving) LTE. In contrast to FeI lines, there is no impact to FeII lines are insensitive to departures from LTE. This is why, the microturbulent velocity ξ_t and the abundance of iron in the atmosphere of a star are determined according to FeII lines.

In the works of Lyubimkov and Samadov [2] it has been proved that, the microturbulent velocity ξ_t increases as the height of atmospheres of F spectral type stars increases. This impact turns even more effective as the line becomes much stronger. For weak lines these dependency is almost insignificant and it is assumed that, microturbulent velocity ξ_t is constant in the atmosphere of the star. While defining microturbulent velocity sufficiently weak lines are only used. These lines emerge in the deep layers of atmosphere, these layers can be regarded as parallel flat layers and LTT condition is met in this case.

Determination of fundamental parameters (T_{eff}, logg) of the star HR7847 (F5Iab) was explained in [3], there diagram defining T_{eff}, logg parameters were specified (Fig. 1). In the diagram fundamental parameters of the stars has been defined as following: $T_{eff} = 6200 \pm 200$K, $\log g = 1.3 \pm 0.2$ According to Kurucz model

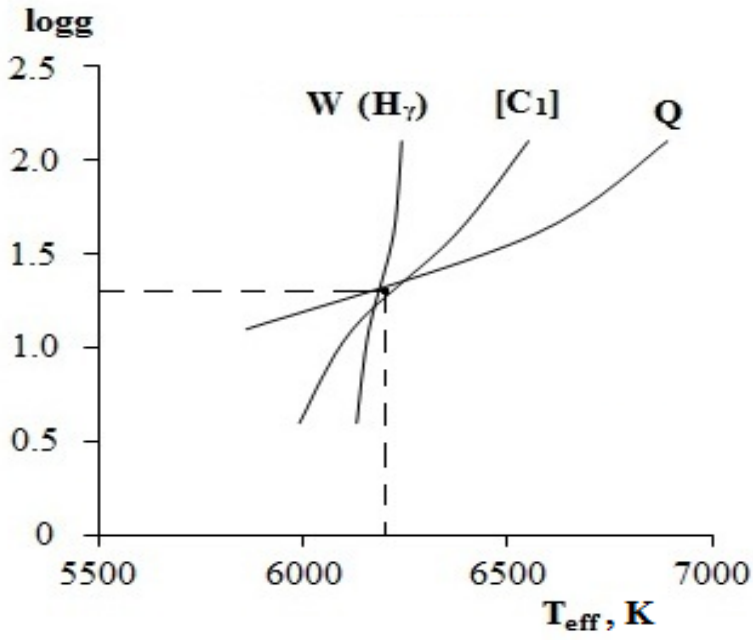

Fig. 1. $\log g - T_{eff}$ diagram

with parameters of T_{eff}=6200K, $\log g$=1.3 [4], the abundance of iron $\log\epsilon$(FeII) is calculated by setting various values to microturbulent velocity ξ_t. The abundance of iron is determined on the comparison of values obtained by observational measurements and theoretical calculations of the equivalent widths of FeII lines. Atomic spectral line data VALD-2 [5] are taken from the database. When ξ_t=5 km/s, there is no correlation between $\log\epsilon$(FeII) and Wλ (Fig. 2). So microtur-

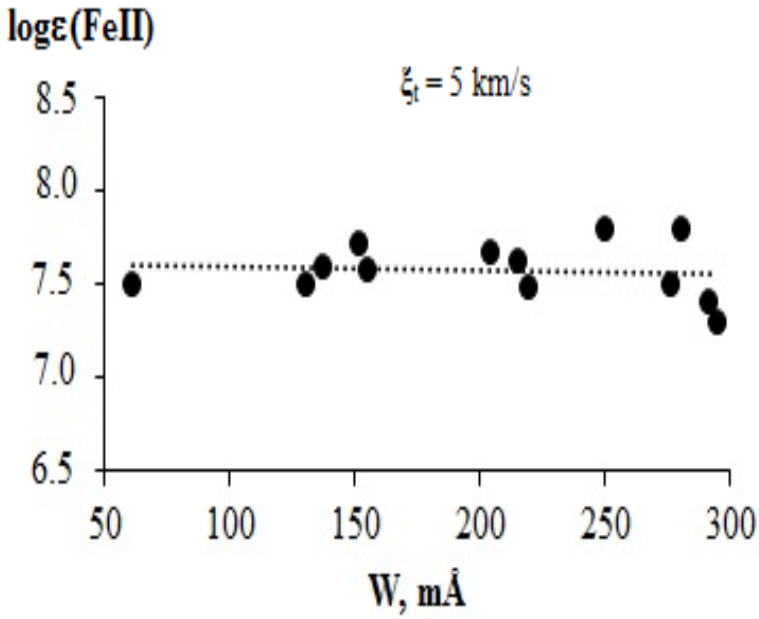

Fig. 2. Determination of microturbulent velocity.

bulent velocity in the atmosphere of the star has been defined to be ξ_t=5 km/s. This value of turbulent motion is almost same with the one obtained by Eggen [6], which is ξ_t=4.0 km/s. With the help of microturbulent velocity we can determine the abundance of iron as well:

$$log\epsilon(Fe) = 7.58 \pm 0.14.$$

$[Fe/H] = \Delta log\epsilon = log\epsilon(Fe) - \log\epsilon_{\odot}(Fe)$ was called is metallicity indicator of the star. $\log\epsilon_{\odot}(Fe)$ in this equation is abundance of iron in the Sun: $\log\epsilon_{\odot}(Fe) = 7.45$, [7]

$$[Fe/H] = 7.58 - 7.45 = 0.13.$$

Among the elements which passed chemical evolution only C and Na elements' lines can be observed on the visible region of the HR7847 star's spectrum. On the basis of these lines abundance of carbon was defined to be:

$$log\epsilon(C) = 7.89 \pm 0.1,$$

and the abundance of sodium was defined to be:

$$log\epsilon(Na) = 6.79 \pm 0.1,$$

$$[C/H] = \Delta log\epsilon = log\epsilon(C) - \log \epsilon_{\odot}(C) = 7.89 - 8.43 = -0.54,$$

$$[Na/H] = \Delta log\epsilon = log\epsilon(Na) - \log \epsilon_{\odot}(Na) = 6.79 - 6.21 = 0.58.$$

Parameters of the star that we have defined are:

$$T_{eff} = 6200 \pm 200K, log = 1.3 \pm 0.2, \xi_t = 5km/s,$$

,

$$log\epsilon(Fe) = 7.58 \pm 0.14, log\epsilon(C) = 7.89 \pm 0.1, log\epsilon(Na) = 6.79 \pm 0.1,$$

$$[Fe/H] = 0.13, [C/H] = -0.54, [Na/H] = 0.58.$$

So, in the atmosphere of F spectral-type star HR7847 the abundance of metals is almost equal to the abundance of metals in the Sun. This indicates that the star HR7847 and the Sun were created in an environment consisting of the same metal substance. This conclusion is important from the standpoint of chemical evolution of Galaxies.

Abundance of carbon in the atmosphere of star HR7847 is less than the abundance of carbon in the Sun, and abundance of sodium in the atmosphere of star HR7847 is more than the one in the Sun. Based on experiments, this conclusion confirms the modern evolutionary theory's clauses.

3. CONCLUSIONS

1. Based on FeII lines, microturbulent velocity has been defined in the atmosphere of the star: ξ_t=5 km/s.

2. Abundance of iron, carbon and sodium in the atmosphere of the star was determined and compared with the abundances of respective elements in the Sun. It has been discovered that, abundance of iron in the star is close to, abundance of carbon is less, and abundance of sodium is more than the abundances of respective elements in the Sun.

Table 1. The list of CI, NaI and FeII lines studied on the spectrum of star HR7847.

λ, Å	n	loggf	W, mÅ	λ, Å	n	loggf	W, mÅ
CI				4384.32	32	-3.68	398
4770.02	6	-2.05	46	4385.38	27	-2.68	3.90
4771.72	6	-1.49	103	4413.59	32	-3.67	219
4775.89	6	-2.01	70	4416.82	27	-2.41	401
4932.04	13	-1.66	32	4472.92	37	-3.53	344
NaI				4489.18	37	-2.97	394
4664.81	12	-1.57	43	4491.40	37	-2.70	398
4668.56	12	-1.30	115	4508.28	38	-2.25	485
FeII				4515.33	37	-2.45	394
4032.94	126	-2.57	276	4520.22	37	-2.607	377
4057.45	212	-1.68	130	4522.63	38	-2.03	621
4087.28	28	-4.52	137	4541.52	38	-2.79	391
4119.52	21	-4.4	155	4549.47	38	-2.02	623
4122.65	28	-3.3	280	4555.89	37	-2.16	551
4124.78	22	-4	250	4576.33	38	-2.92	365
4128.74	27	-3.58	311	4580.05	26	-3.90	291
4138.40	39	-4.31	151	4582.83	37	-3.09	364
4173.45	27	-2.74	546	4583.83	38	-1.86	619
4178.85	28	-2.5	513	4620.51	38	-3.24	300
4233.17	27	-1.90	295	4629.34	37	-2.33	426
4258.15	28	-3.48	485	4656.97	43	-3.61	363
4273.32	27	-3.30	351	4663.70	44	-3.71	215
4278.15	32	-3.95	204	4666.75	37	-3.83	308
4296.57	28	-2.93	403	4670.17	25	-4.06	353
4303.17	27	-2.56	457	4731.14	43	-3.02	304
4351.76	27	-2.02	546	4893.78	36	-2.56	77
4357.57		-2.01	61	4923.92	42	-1.32	341
4369.40	28	-3.58	300				

REFERENCES

1. Boyarchuk A.A., Lyubimcov, L.S. Detalniy analiz sverkhgigantov classa F. II. Raspredelenie microturbulentnosti i soderjanie elementov v atmosfere ρ Cas. 1983, Izv. CrAO, 66, 130 (in Russian).

2. Lyubimkov, L.S., Samedov, Z.A. O peremennosti mikroturbilentnosti v atmospherakh - F sverkhgigantov.1990, Astrophizika, 32, 49 (in Russian).

3. Samedov, Z.A., Khalilov, A.M., Hasanova, A.R., Samadova, N.H. Determination fundamental parameters of the star of 44 Cyg (F5Ib). 2012, AJA, 2, 13 (in Azerbaijani)

4. Kurucz, R.L. ATLAS9, Stellar Atmosphere Programs and 2km/s grid., Cambridge, USA, Mass.;Smithsonian Astrophysical Observatory, 1993, CD-ROM №13

5. Kupka, F., Piskunov, N., Ryabchikova,T.A., Stempels, H.C., Weiss,W.W. VALD2: Progress of the Vienna Atomic Line Data Base. 1999, A&AS, 138, 119

6. Eggen, O.G. Photometry of F-K type bright giant and supergiants. II-Calibration on indices in terms of luminosity reddening and abundance of F-type stars. 1991, AJ, 102, 1826

7. Scott, P., Asplund, M., Grevesse, N., Bergemann, M., Jacques Sauval, A. The elemental composition of the Sun. II. The iron group elements Sc to Ni, 2015, A&A, 26, 573

HR 7847(F5Iab) ULDUZUNUN ATMOSFERİNDƏ METALLIĞIN, KARBON VƏ NATRİUM ELEMENTLƏRİNİN MİQDARININ TƏYİNİ

***Z. A. Səmədov*[a,b], *Ə. M. Xəlilov*[a], *Ə. R. Həsənova*[a], *Ü. R. Qədirova*[a], *G. M. Hacıyeva*[a], *N. H. Səmədova*[a]**

[a] *N.Tusi adına Şamaxı Astrofizika Rəsədxanası, Azərbaycan Milli Elmlər Akademiyası, Şamaxı rayonu, Azərbaycan*
[b] *Bakı Dövlət Universiteti, Bakı, Azərbaycan*

HR7847 (F5Iab) ulduzunun Şamaxı Astrofizika Rəsədxanasının 2 m teleskopunun Kude fokusunda 8 Åmm dispersiya və 0.3Å spektral ayırdetmə ilə alınmış spektrləri tədqiq edilmişdir. FeII xətləri əsasında ulduzun atmosferində mikroturbulent hərəkət sürəti təyin edilmişdir: ξ_t=5.0 km s^{-1}. Ulduzun atmosferində dəmir, karbon və natrium elementləriniin miqdarı təyin edilmişdir. Aşkar edilmişdir ki, Günəşin kimyəvi tərkibi ilə müqayisədə karbon elementinin miqdarı az, natrium elementinin miqdarı isə çoxdur. Dəmirin miqdarı Günəşdəki miqdara yaxındır.

Açar sözlər: Ulduzlar: fundamental parametrlər - Ulduzlar: kimyəvi tərkib – Ulduzlar: fərdi - HR7847 (F5Iab)

ON THE SPIRAL STRUCTURES IN HEAVY-ION COLLISIONS

J. N. Rustamov [a], ***A. J. Rustamov*** [b,c,d]

[a] *Shamakhy Astrophysical Observatory named after N.Tusi, Azerbaijan National Academy of Sciences, Shamakhy region, Azerbaijan*

[b] *GSI, Helmholtzzentrum fur Schwerionenforschung, Darmstadt, Germany*

[c] *Physikalisches Institut, Universitatat Heidelberg, Heidelberg, Germany*

[d] *National Nuclear Research Center, Baku, Azerbaijan*

It is well established that many galaxies, like our Milky Way, exhibit spiral patterns. The entire galactic disc rotates about the galactic centre with different speeds; higher closer to the centre, lower at greater distances - that is, galactic discs do not rotate like a solid compact disc. The spiral arms are the part of the galactic disc where many young stars are being born. Since young stars are also brightest, we can see the spiral structure of other galaxies from afar. Typically spiral galaxies are copiously observed at redshirts z $\sim$ 1. The recently observed grand-design spiral galaxy Q2343-BX442 at z = 2.18, however, implies uncertain origin of its spiral structure [1]. Indeed such "old" galaxies usually look rather clumpy because of their dynamically hot discs. In this report, based on self-similarity, we argue that spiral structures may also appear in heavy-ion collisions as messengers of phase transitions. Thus, spiral structures in galactic patterns may be traced back to a few microseconds after the Big Bang.

1. INTRODUCTION

To our knowledge, Rolf Hagedorn was the first to consider the concept of self-similarity in particle physics, which ultimately led to the concept of limiting temperature and phase transitions in the strongly interacting matter [2–5]. His main idea was to search for self-similar patterns in the composition of heavy particles; heavy particles are composed of lighter ones, and these again in turn of a still lighter one, until one reaches a fundamental constituent, which in his case was a pion, the lightest hadron [6]. Mathematically the problem is formulated

with the following bootstrap equation [7]:

$$\rho(m,V_0)=\delta(m-m_0)+\sum_{N=2}^{\infty}\frac{1}{N!}[\frac{V_0}{(2\pi)^3}]^{N-1}\prod_{i=1}^{N}\int dm_i\rho(m_i)\rho(m_i)\int d^3\rho_i\delta^4(\sum_i\rho_i-\rho) \tag{1}$$

Here the first delta function represents pion, while the last four-delta function guaranties the 4-momentum conservation. The solution of the bootstrap equation is given in Ref. [8] :

$$\rho(m,V_0)\sim m^{-3}e^{m/T_H}, \tag{2}$$

where T_H is referred to as the Hagedorn limiting temperature. By taking the composition volume V_0 to be spherical with the radius of inverse pion mass Hagedorn got a value of about 150 MeV for the limiting temperature T_H.

The self-similar properties of the Hagedorn fireballs within the statistical-bootstrap model were formulated by Frautschi [7] who used Eq. 1 to describe the fireball decay. For a heavy fireball, $m \gg m_0$, the probability distribution P(n) of its one-step decay into n lighter fireballs ($n \geq 2$) appears to be independent of m and has the form:

$$P(n)=\frac{(ln2)^{n-1}}{(n-1)!}. \tag{3}$$

This equation shows that dominant channels correspond to 2-body decays with P(2)$\cong$ 0.69 and 3-body decays with $P(3) \cong 0.24$. If an m_1 and m_2, which are the decay products in a reaction $m \to m_1 + m_2$, are also heavy Eq. 3 applies in this case as well. Original fireball with mass m and its constituents m_1 and m_2 have the same properties provided that all these masses are much larger than m_0 and T_H. Therefore, one finds a similar behavior for the whole system m and for its part m_1, that is what self-similarity stands for.

2. MOST POPULAR SELF-SIMILAR OBJECTS

Any object is said to be self-similar if it is reproduced by magnifying some part of it. Self-similarity can manifest itself both in discrete and continuous fashion, albeit in most cases the exact self-similarity is only asymptotically so. A well-known example of a discrete self-similarity is Russian dolls where a larger doll discretely hides a similar smaller one inside it and so forth. If we had infinite number of dolls, both ever smaller and ever larger, we would have a set with exact discrete self-similarity. The obvious limitation on the size of the dolls from both sides makes this discrete self-similarity only approximate. Another charming and copiously encountered in nature example of a self-similar object is the logarithmic spiral. In polar coordinates the equation of the logarithmic spiral is given as:

$$r(\phi) = r_0 e^{k\phi}, \tag{4}$$

where r_0 and k are constants. Scaling the spiral by a factor s is equivalent to the same spiral rotated by a constant angle of $ln(s)/k$:

$$sr(\phi) = sr_0 e^{(k\phi)} = r_0 e^{ln(s)} e^{k\phi} = r_o e^k (\phi + \frac{ln(s)}{k}). \tag{5}$$

For a particular value of $s = e^{2\pi km}$, with m being any integer number, one gets the same spiral rotated by an angle:

$$ln(e^{2\pi km})/k = 2\pi m. \tag{6}$$

As in the case of Russian dolls, the exact self-similarity for the logarithmic spiral is limited by finite the value of r_0 (see. Eg. 4) and the size of the spiral.

3. SPIRAL STRUCTURES IN STRONGLY INTERACTING MATTER

In non-central high energy heavy-ion collisions large orbital angular momenta are developed, with its vector directed perpendicularly to the reaction plane. The latter is defined by the beam direction and the impact parameter. A fraction of the angular momenta is taken away by the spectators, though the strongly interacting matter in the overlap region will also carry substantial orbital angular momenta. For instance, in non-central $Au + Au$ collisions at RHIC energies the global angular momentum of the overlapping matter was estimated to be of the order of 10^5 spin units [9]. Consequently, the produced matter will rotate. This should be manifested as polarizations of the produced spin non-zero hadrons. In particular, polarizations of vector mesons and hyperons are expected. On the other hand, a correlation length diverges near the critical point, and the matter has to rotate only in a scale invariant, i.e., self-similar way. This scenario can be achieved if rotations follow a logarithmic spiral mentioned in the previous section [10].

4. PROPOSED MEASUREMENTS

Obviously, the spiral structures described in the previous section develop in the coordinate space. On the other hand, the information available from the experiments are in the momentum space. If particles are indeed moving along the spiral structure in the coordinate space, their momentum vectors will be directed along the tangent to the spiral at the given point. One of the many remarkable features of the logarithmic spiral is that the angle between the tangent to the

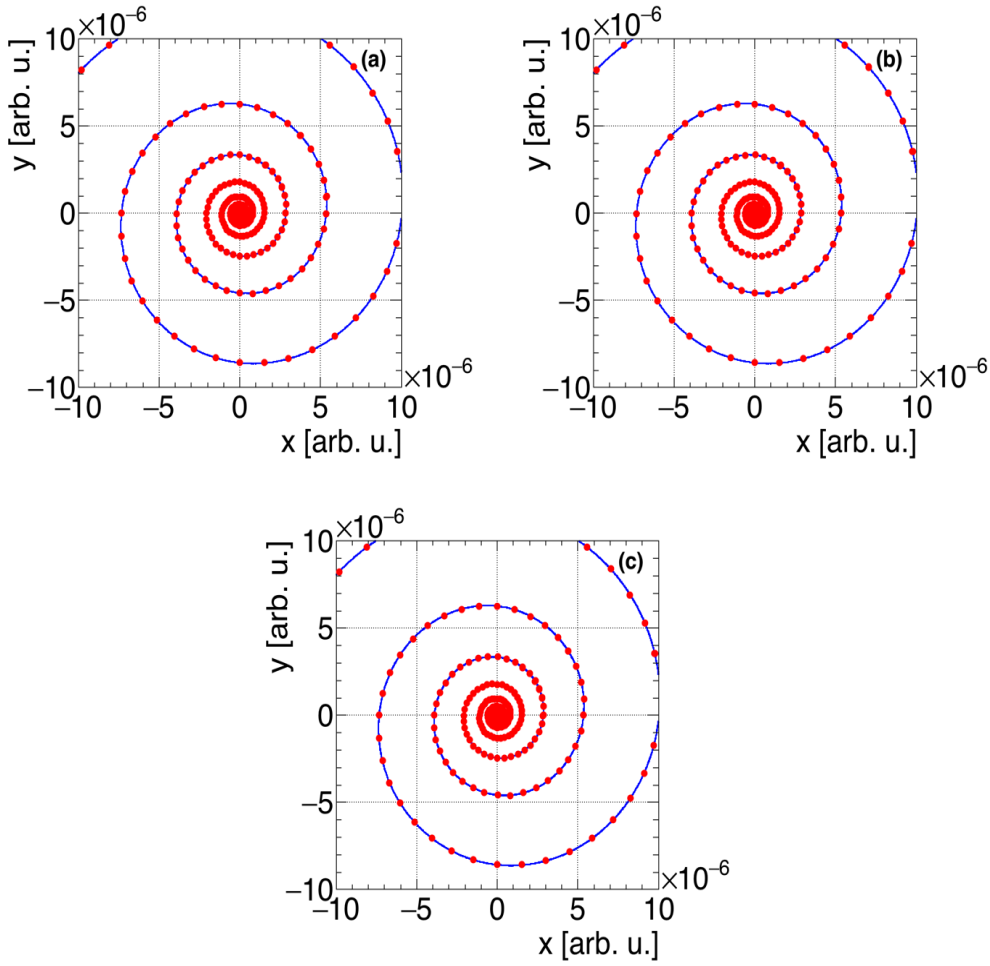

Fig. 1. Color online. Panel (a): A logarithmic spiral as defined in Eq. 4 with $r_0 = 10^{-8}$ and k=0.1 is plotted with the blue line. Red points are generated in flat azimuthal angle along the spiral. In panels (b) and (c) the spiral is scaled with a factor of $s_1 = e^{2\pi}$ and $s_2 = e^{4\pi}$, correspondingly. These scalings do not change the overall distribution of the red points

spiral and the radius vector is always constant and independent of the position on the spiral.

Hence the spiral structure should also evolve into the momentum space. Furthermore, the distribution of particles along the spiral should not destroy she self-similarity pattern, which puts strict limitations on this distribution. It is easy to note that the only possibility to preserve the self-similarity feature of the logarithmic spiral is to distribute points uniformly in azimuthal angle as plotted

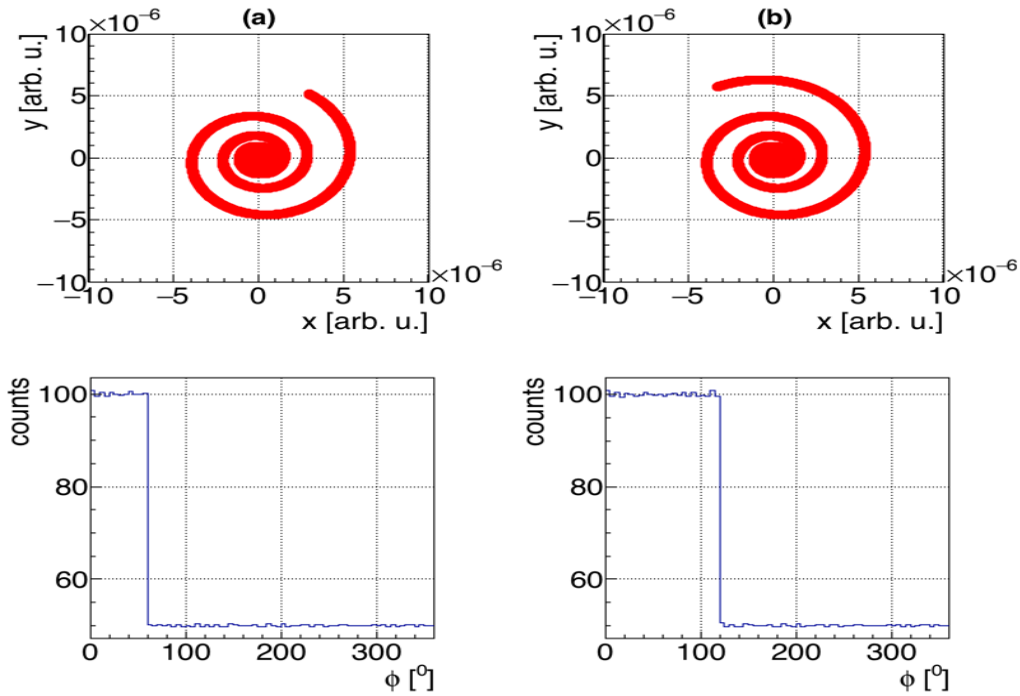

Fig. 2. Color Online. Upper panel: The distribution of points along the spiral, generated in flat azimuthal angle, is illustrated for two different orientations of the spiral. Lower panel: The corresponding angular distributions are shown.

in Fig. 1.Because of the finite size of the system, the spiral will also have a finite size and could be encoded in the azimuthal distribution of the produced particles. This is illustrated in Fig. 2 for two different orientations of spirals. It is obvious that the orientation of spirals will change from event-to-event, the objective is to search for event-by-event fluctuations in the azimuthal distributions of particles in the reaction plane. Spiral structures can also be looked at by plotting the logarithm of Eq. 4:

$$ln(r(\phi)) = ln(r_0) + k \times \phi \tag{7}$$

In this representation the equation of the logarithmic spiral translates into straight lines as demonstrated in Fig. 3. On the left panel of Fig. 3 the points are distributed along the spiral generated from Fig. 1 with r_0 and k parameters taken to be 10^{-6} and 0.06 respectively, while on the right panel the same spiral is represented with Eq. 7. Next, we introduce random background by sampling the points from the uniform distribution superimposed with the points from the spiral, randomly generated from Fig. 1, although with different point densities.

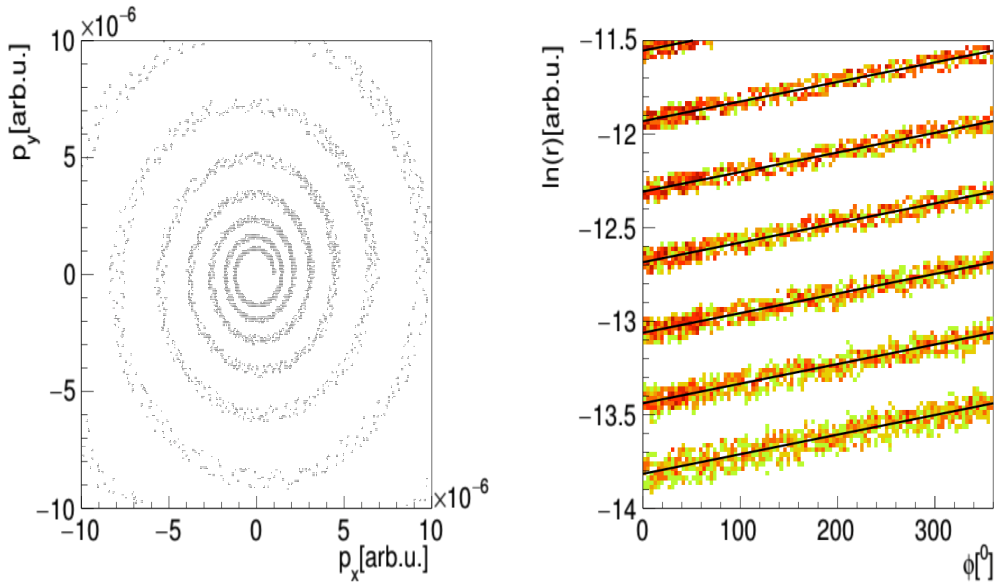

Fig. 3. Color Online. Left panel: The distribution of points along the spiral sampled from Fig. 1 with $r_0 = 10^{-6}$ and k=0.06. Right panel: The corresponding representation with Eq. 7

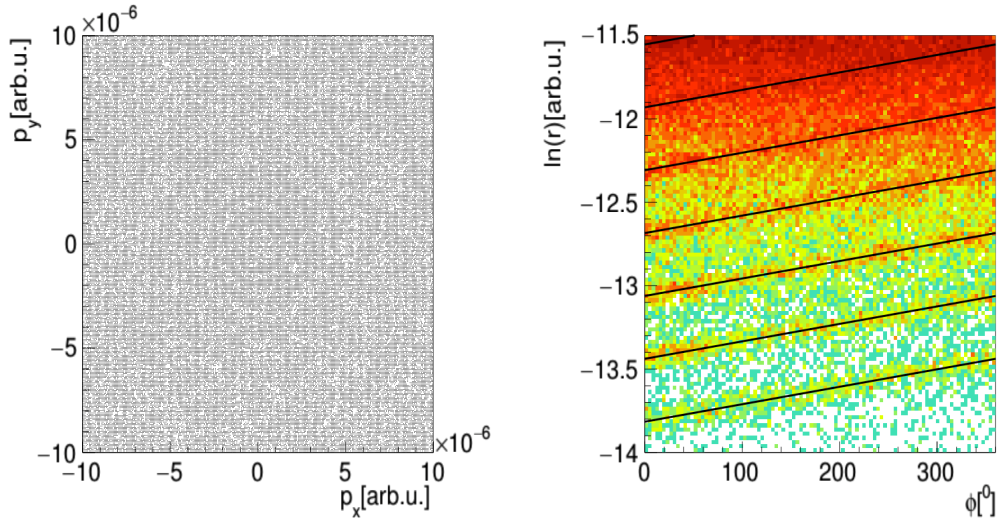

Fig. 4. Color Online. Left panel: Random background points sampled from the uniform distribution superimposed with the points from the spiral. The background is taken to be 10 times larger than the signal (see text for details). Right panel: The corresponding representation with Eq. 7.

Moreover, the background is taken to be 10 times larger; at each 10^{th} sample of the background a random point from the spiral is added. The obtained pattern is presented in the left panel of Fig. 4 The corresponding representation with Eq. 7 is demonstrated in the right panel of Fig. 4, where the spiral structures can still be distinguished. The solid black lines in the right panels of Figs. 3 and 4 correspond to analytical calculations with Eq. 7.

5. CONCLUSION

In summary, near the critical point, spiral structures should appear in the non-central heavy-ion collisions. This scenario may arise when combining two distinct arguments on non-vanishing orbital angular momentum in heavy-ion collisions and well-known phenomenon of the divergence of the correlation length near the critical point. While the first argument leads to the overall rotation of the system in the reaction plane, the second one requires the scale invariance, i.e., self-similarity of the system. The logarithmic spiral satisfies both of these requirements. On the other hand, the constant shape of the logarithmic spiral reveals itself in nature at all scales; from unicellular foraminifera, nautilus shell, sunflower seeds up to giant structures in the Universe. One can argue that these structures may be artefacts of successive phase transitions the Universe passed through during its first moments.

ACKNOWLEDGMENTS

A.R. acknowledges stimulating discussions with Marek Gazdzicki, Mark Gorenstein and Oleg Teryaev.

REFERENCES

1. David R. Law et al. High velocity dispersion in a rare grand-design spiral galaxy at redshift z = 2.18. 2012, NATURE, 487, 338 [doi:10.1038/nature11256]

2. Hagedorn, R. Statistical thermodynamics of strong interactions at high energies. 1965, Nuovo Cim. Suppl. 3, 147

3. Hagedorn, R. & Ranft, J. Statistical thermodynamics of strong interactions at high-energies. 2. Momentum spectra of particles produced in pp-collisions. 1968, Nuovo Cim. Suppl. 6, 169

4. Hagedorn, R. Statistical thermodynamics of strong interactions at high energies. 3. Heavy-pair (quark). 1968, Nuovo. Cim. Suppl., 6, 311

5. Hagedorn, R. Hadronic matter near the boiling point. 1968, Nuovo Cim. Suppl., A56, 1027 [doi:10.1007/BF02751614]

6. Redlich, K. & Satz, H. The Legacy of Rolf Hagedorn: Statistical Bootstrap and Ultimate Temperature. 2015, arxiv: 1501.07523 [doi: 10.1007/978-3-319-17545-4_7]

7. Frautschi, S. Statistical Bootstrap Model of Hadrons. 1971, Phys. Rev., D 3, 2821 [doi:10.1103/PhysRevD.3.2821]

8. Nahm, W. Analytical solution of the statistical bootstrap model. 1972, Nuclear Phys. B. 45, 525 [doi: 10.1016/0550-3213(72)90257-X]

9. Liang, Z. Global polarization of QGP in non-central heavy-ion collisions at high energies. 2007, J. Phys. G: Nucl. Part. Phys., 34, 8

10. Rustamov, A.J., Rustamov, J.N. On the Spiral Structures in Heavy-Ion Collisions. 2016. arxiv: 1602.01812

RESULTS OF LONG TIME SPECTRAL MONITORING OF THE STAR IL CEP A

N. Z. Ismailov [a], ***M. A. Pogodin*** [b], ***U. Z. Bashirova*** [a],

G. R. Bahaddinova [a]

[a] *Shamakhy Astrophysical Observatory named after N.Tusi, Azerbaijan National Academy of Sciences, Shamakhy region, Azerbaijan*

[b] *Astronomical Observatory (Pulkovo) of Russian Academy of Sciences, Pulkovo, Russia*

The results of long-time spectral observations of the Be Herbig star IL Cep A are presented. For the first time, a smooth variation in the radial velocities of the emission component in the Hα and Hβ hydrogen lines was discovered. The radial velocities for the lines D NaI and DIB λ5780, 5796 Å correspond to the radial velocities of the interstellar medium. It is shown that hydrogen emission lines, are formed in the disk, rather is formed only around one of the components of the binary system. The orbital elements of the system were calculated in the spectral binary star model with a period of 3550 $\pm$ 28 days. It was estimated fundamental parameters of the individual components of the system. It is assumed that the secondary component of the system is a young star with a circumstellar disk.

Keywords: tars– Young binary stars–Spectral variability, Ae/Be Herbig type stars– IL Cep A.

1. INTRODUCTION

The Herbig Ae/Be type stars (HAeBes) are young objects of intermediate masses (2-10 $M_\odot$) and are at the evolutionary stage to the Main Sequence (MS). These stars mainly have spectral classes B-A, luminosity types IV-V, and strong emission lines are observed in their spectrum. These stars are often located in dark clouds, associated with bright reflective nebulae and have strong infrared (IR) excess radiation (see, for example, [1–3]). It is currently accepted that HAeBes are an intermediate mass stars between T Tauri stars and more massive stars. Like the classic T Tauri stars (CTTS), HAeBes stars are surrounded by a circumstellar

residual gas-dust disk. The disk re-emits the radiation of the central star and is a source of thermal radiation in the infrared range.

To date, direct images of the circumstellar disks structure have been obtained for some objects [4,5]. Circumstellar disks have a complex structure, and, apparently, the accretion of matter from disk to the star plays a significant role in the variability of the spectrum and brightness of the star. Therefore, the study of the emission spectrum of HAeBes could shed light on the nature of the interaction between the central star and the circumstellar disk.

The star IL Cep (HD 216629) is visually binary with the components IL Cep A ($\alpha_{2000} = 22^h53^m15.603^s$, $\delta_{2000} = +\ 62°08'45.02'$, V$\sim$ 9.36 mag) and IL Cep B ($\alpha_{2000} = 22^h53^m15.342^s$, $\delta_{2000} = +\ 62°08'51.629$", V $\sim$ 13.82 mag) and with angular distance 6."96 [6]. The system is known as a member of the young association Cep OB3. Wheelwright et al. [7] showed that the star IL Cep A also has a closer visual component at an angular distance of 0."44 , which is weaker than IL Cep A at ΔB = 3.5 mag. Obviously, with such a close companion brightness, the contribution of its radiation to the spectrum of the star IL Cep A will be insignificant. Considering this circumstance in the future in our work we will discuss only on the component IL Cep A.

According to Assousa et al. [8] IL Cep is an emission object closely related to the reflection nebula, and therefore is an Ae/Be Herbig type star. According to [9] and [10], the star belongs to the Cep OB3 association. However, as is shown in [11], using the distance to the star at 720 ps (see, for example, [12]), the star will take a position below the ZAMS (Zero Age Main Sequence) line on the evolutionary HR diagram. Since the star is a visual binary system, in [11] the authors did not estimate its fundamental parameters using evolutionary tracks.

Hill [13] established the periodic variability of the brightness of the star with a period of 1.401 days, which, according to the author, could be caused by eclipses in a binary system. Therefore, the star was included in the GCVS [14] as an eclipsing type EA. Later, the periodicity was not confirmed, although the variability of the brightness of the star was not in doubt [15]. Further analysis of the photometric data of Mel'nikov et al. [16] showed that it is possible that the star's brightness varies with a period of 50.91 days with a minimal amplitude of ΔV = 0.03 mag.

According to different authors, the spectrum of the star was defined as B2IV-V [10], B3e [17], B0, B3, B2 ([9] and in references therein). According to calculations in [11], the spectrum of the star can be represented by a combination of the spectra of two stars with components B3 and B4. The authors showed that the radial velocities (RV) of the stars given in the literature differ from -39.4 km/s to 31 km/s [10], [11], [16]. According to the interstellar absorption lines of CaII for RV it was obtained from -11 km/s to -19 km/s [10], [16]. Long-term spectral

observations have shown that the radial velocities of the emission component of the hydrogen lines Hα and Hβ show smooth long-term variations [18], [19]. The radial velocities of the D Na I lines generally agree with the velocities of the interstellar absorption lines; at the same time, there is a certain contribution to these lines of circumstellar gas [18]. The measurements of the radial velocities showed that the star may be spectrally binary with a period of about 10 years [19]. Recently in the work [20] it was shown that the emission spectrum of a star can be described by radiation of the circumstellar envelope with a radius of 25 R_* under the action of photoionization radiation of the B2 star.

Some authors obtained a significant scatter of the values of equivalent widths (EW) of the Hα line: 10 Å [21], 21 Å [16], 8 Å [7], 34.5 Å [20]. The Hα line profile is observed to be two-component, with slightly separated peaks, and the Hβ line shows two confidently separated peaks and a central absorption (see, for example, [19, 23],). Our measurements showed the existence of minor seasonal changes in the equivalent widths of the hydrogen lines, but these changes did not show a correlation with changes in the radial velocities of the star. In this paper, we presents the results of research of the spectrum IL Cep A, using also the new spectral material obtained in 2015-2017.

2. OBSERVATIONS

Spectral observations were performed in 2006–2017 in the Cassegrain focus of the 2 m telescope of the Shamakhy Astrophysical Observatory of the Azerbaijan National Academy of Sciences (ShAO of ANAS). Two spectrometers were used: the first spectrometer (MUAGS – Modified Universal Astronomical Grid Spectrograph) was used in 2006-2015, which was made on the basis of the UAGS spectrograph [24], [19].

A CCD matrix with 530×580 elements, cooled with liquid nitrogen, was applied to the first spectrograph. The matrix had a linear dimension of 9.5×13.9 mm. The size of one pixel is 18×24 microns. The inverse linear dispersion in the red part is 10.5 Å/mm, and in the blue part about 6 Å/mm. The entire observed area can be covered in two steps. The observations of the star IL Cep were performed in the red part of the spectrum, which covers the range of λ 4700-6700 Å. Most of our spectral material was obtained on this spectrograph (2006-2015).

The spectral resolution of this spectrograph was R = 14000; the signal-to-noise ratio in the region of the Hα line is S/N = 80–100, and in the region of the Hβ line is S/N = 10-20. All image processing, their processing into a standard format, and further measurements of spectrograms were performed using the DECH20T program developed at the SAO RAS [25].

The ShaFES Fiber Echelle spectrograph (Shamakhy Fiber Echelle Spectrograph) consists of two parts: the first part is the spectrograph itself, which is installed in a thermostatically isolated room on a rigid supply. The second part with the light emitting device is mounted on the Cassegrain focus. These systems are connected by a light fiber cable with a diameter of 200 μm and a length of 20 m. The spectrum in the focal plane of the spectrograph chamber is projected onto a CCD matrix with 4K×4K elements cooled by liquid nitrogen. The pixel size is 15 μm, the maximum quantum yield at a wavelength of 4000 Åis 90%. A detailed description of the ShaFES spectrograph is given in Mikayilov et al. [26]. The spectral resolution depending on the selection of pixel dimensions is 1 px = 15 μm obtained R = 56000 for and 1 px = 30 μm obtained R = 28000. With such resolutions, it is possible to obtain the spectra of stars up to 8 and 10 magnitudes, respectively. The linear dimensions of a CCD of 61x61 mm make it possible to cover the range λ 3800-8500 Å. For IL Cep spectra were obtained at a resolution of R = 28000, in the range of 3900-7500 Å. For the reduction and processing of the spectrograms, the DECH95 and DECH30 programs developed by Galazutdinov were used (http://www.gazinur.com/Image-Processing-.html). For monitoring the stability of the system on each night of observations, standard star spectra, a flat field image and a comparison spectrum were obtained. For the reduction of wavelengths, the spectrum of the sky and the spectrum of the lamp ThAr were used. The spectral parameters of the lines were regularly measured using selected lines of the spectrum of standard stars and the sky spectrum. Systematic measurements of selected lines show that with a resolution of R $\sim$ 14000, the FWHM half-width of single atmospheric lines provides good stability within the standard deviation of $\pm$ 0.04 Å.

The measure of the instrumental contour for the MUAGS spectrograph was performed using the spectral lines of the spectrum of a ThAr lamp in the blue and red parts, which turned out to be 0.36 Åand 0.44 Å, respectively. The average value of the instrumental contour along the intense argon line λ 6032.124 Åturned out to be 0.44 $\pm$ 0.04 Å, which can be taken as the upper limit of this parameter [18]. The half-width of the instrumental contour for the ShaFES spectrograph was approximately half as large.

According to spectrograms of standard stars HR7300 (G8II-III) and HR 7794 (G8III-IV) obtained under the same conditions, it is shown that the results of 14 nights of observations vary the standard deviation of equivalent widths from 12% to 3.5% for lines with an average EW from 0.05 Å to 0.5 Å, respectively. Our measurements showed that the average measurement error of the EW parameter of the central emission in the Hα line does not exceed 5%.

The control measurements of radial velocities for various standard stars showed a high degree of coincidence of measured RV values with data from the catalog

within measurement errors of ± 3 km/s. There was no systematic difference in our RV measurements by standard stars within the measurement errors. The radial velocities from the spectra of the ShaFES spectrograph were measured with an accuracy of about ± 1 km/s.

The log of observations is given in Table 1, where in the columns from left to right is given the interval of the date of observations in each year, N is the number of spectrograms obtained, the number of nights of observations per year, the exposition time in seconds, the signal-to-noise ratio S/N about the Hα line, the type of spectrograph and spectral resolution. The observation was carried out in just 58 separate nights. Each pair of spectra obtained for individual nights was averaged. In 2012, no observations were made due to the repair of the 2 m telescope. On some nights, 2–3 pairs of spectrograms of the star were obtained, and the measured parameters were also averaged over them during the night of observations.

Table 1. Log of spectral observation IL Cep

Observation dates	N	nights	Exposition, sec	S/N at Hα	Spectrograph	R=$\lambda/\Delta\lambda$
12 August -19 August 2006	8	4	1500	100	MUAGS	14000
20 August 2007	2	1	2400	110	MUAGS	14000
04 August -25 August 2008	10	5	1800	110	MUAGS	14000
08 July – 25 October 2009	22	11	2600	95	MUAGS	14000
01 August -16 November 2010	24	12	3600	120	MUAGS	14000
07 November 2011	2	1	3600	110	MUAGS	14000
25 August -17 October 2013	12	6	2400	90	MUAGS	14000
24 July – 28 August 2014	14	7	3600	115	MUAGS	14000
20 June – 06 September 2015	16	8	3600	110	MUAGS	14000
13 July -19 august 2016	4	2	3600	90	ShAFES	28000
28 July 2017	2	1	3600	80	ShAFES	28000

3. VARIABILITY OF THE LINE PARAMETERS

As shown in our previous works , the Hα line has a strong emission profile with two peaks [18], [19]. On some days there is a single peak. To measure the radial velocities of the Hα emission line, we first measured the displacement of the center of the line relative to the wings at the level of half the total intensity (bisector velocity, RVb).

Fig. 1 shows graphs of the equivalent widths and radial velocities variations of the Hα line for all spectrums, obtained to date. As seen from Fig. 1, the radial

velocities show a smooth sinusoidal change from +10 to -70 km/s, indicating that possible the star is spectroscopic binary. The values of EW show a variability of approximately ± 2 Ånear the mean value of 12 ± 0.6 Å. At the same time, there is no definite correlation in the changes between the RV and EW parameters.

Fig. 2 shows the time variations in FWHM (half-widths) of Hα emission. As one can see, there is a seasonal variation of this parameter, but no synchronic with changes in RV is detected (Fig. 1 , right panel). If the system will be consisted of two stars each with of individual discs, then we would be detected a periodic variation in this parameter.

Unfortunately, in the spectral range of the star that we obtained, to measure the radial velocities of the individual components of the system no any clean origin photosphere absorption lines were observed. The strongest absorption lines in the spectrum of the star in the range λ4700-6700 Åare the lines He I λ 5876 Å, D1, D2 NaI, and the interstellar absorption band DIB 5780, 5796 Å [19]. As shown in [27] and [28], the line He I λ5876 Åin the spectrum IL Cep A has a complex multicomponent structure, and possibly contains a hidden emission component. From the change in the parameter RV in this line, the root-mean-square scattering of the order of ± 11 km/s was obtained, around the mean value of -17 km/s. For variations in the parameter EW, 0.56 ± 0.16 Åwas obtained. The He I λ 5876 Å line may be partially formed in the shock wave in the zone of disk accretion, or it may be distorted by additional emission generated in the circumstellar disk. Therefore, if even in this line there is a contribution to RV due to the orbital motion of the main component, then this contribution cannot be distinguished by the complex structure of the line.

The D1, D2 NaI lines show insignificant variability, and rather, they are partially formed in the circumstellar disk and in the interstellar medium [18]. The average value of radial velocities along the lines D1 and D2 obtained -11.7 ± 1.9 km/s and -11.9 ± 1.6 km/s, respectively. The same RV values were obtained for interstellar absorption bands DIB λ 5780, 5796 Å. It follows that if the system is immersed in a nebula, the velocity of the center of mass of the observed spectrum of the B2 star should be about -11 km/s. According to [29] for the IL Cep radial velocity of the circumstellar lines is equal to -10 km/s, which confirmed well with our data.

For the consideration of the question of duplicity, we additionally measured bisector radial velocities along the Hα emission profile at the levels of 1.00Ic, 1.25Ic, 1.50Ic, 1.75Ic, 2.00Ic, where Ic is the intensity of the continuum. We proceeded from the assumption that at intensity levels close to the level of the continuous spectrum, emission wings form in the inner layers of the accretion disk, which has axial symmetry about the center of the star. Therefore, the value of Vbis must correspond to the radial velocity of the star itself. Such an assumption was used

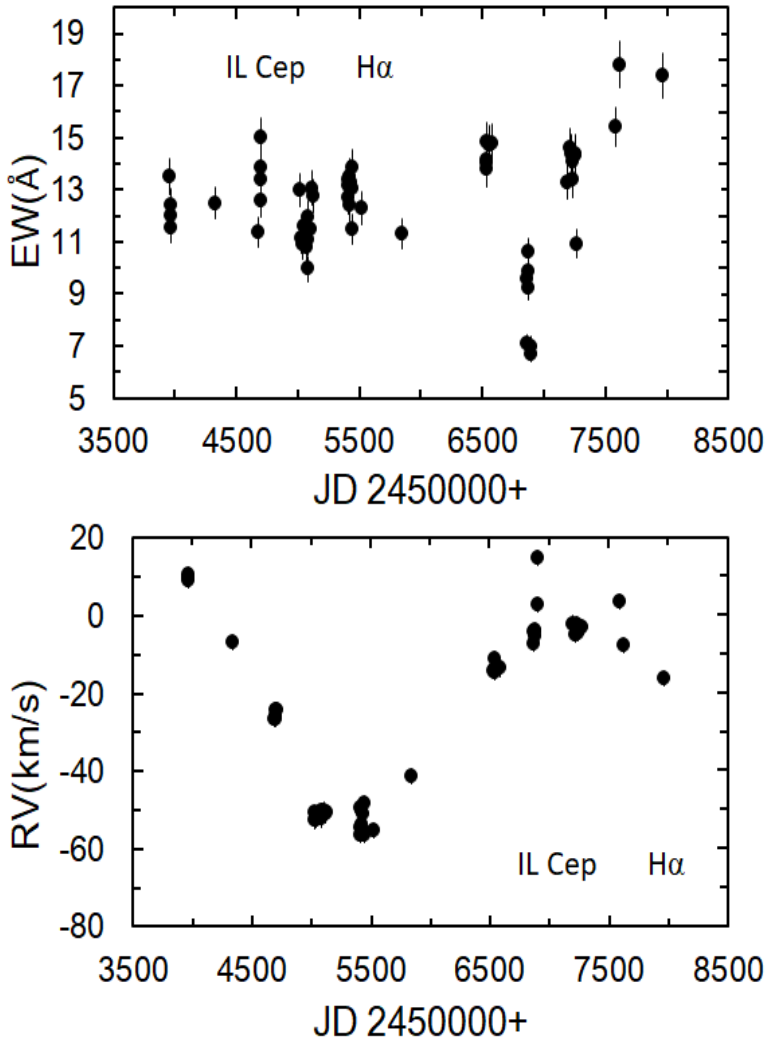

Fig. 1. Time variations of the EW (left) and RV (right) emission line Hα.

in [30] devoted to the determination of the orbital elements of the spectral binary Be Herbig star HD200775.

Our measurements of radial velocities at different intensity levels showed that the best agreement with the obtained Vbis curves was obtained at the continuum level of 1.00Ic to 1.50Ic. At higher intensity levels, the spread of points increases significantly. In Fig.3 was shown the radial-velocity curve obtained at three different levels of intensity — 1.0Ic, 1.5Ic and 1.75Ic. As can be seen from here, the scatter of points for individual seasons of observations ranges from 10 to 15 km/s. But the average annual value of Vbis smoothly varies from +5 to - 80 km/s.

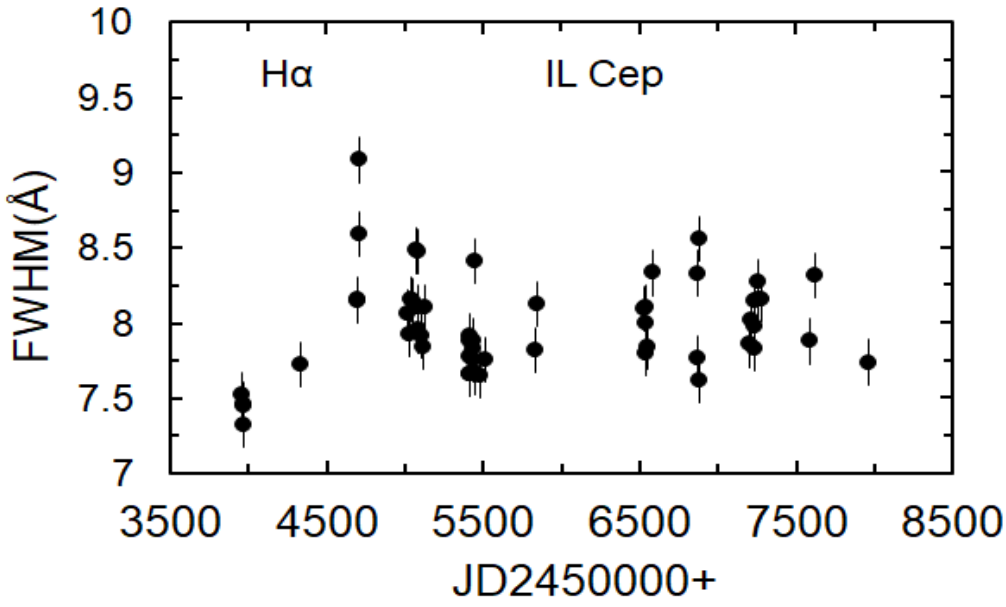

Fig. 2. Time variations of the parameter FWHM of the emission line Hα.

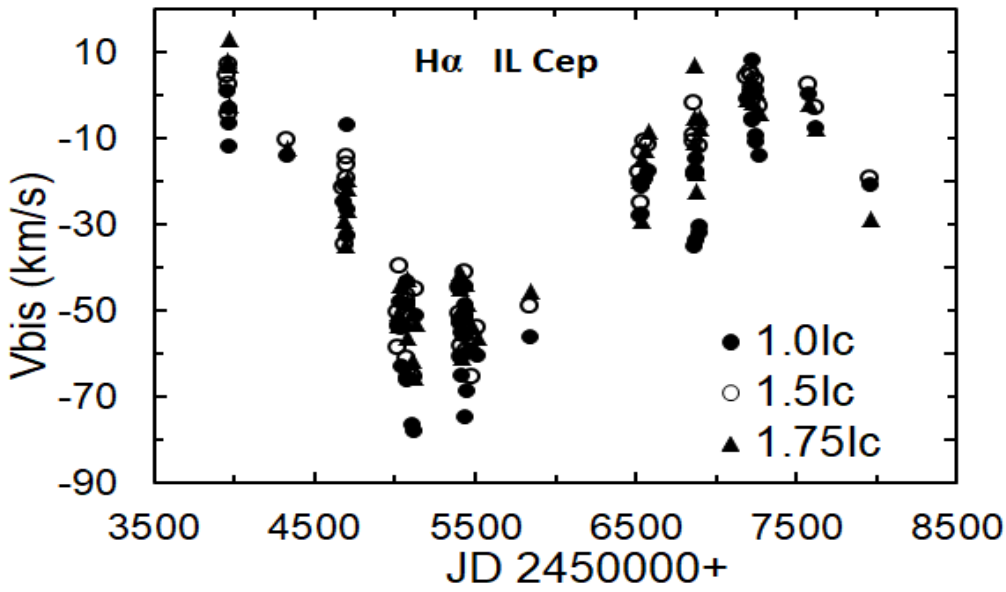

Fig. 3. The radial-velocity curves for the Hα line at different intensity levels: 1.0lc - dark circles, 1.5lc - light circles, and 1.75lc - triangles.

4. DETERMINATION OF THE ORBITAL ELEMENTS

The method of our calculations is based on a comparison of the observed phase curve for a predetermined value of the orbital period P with a theoretical curve for the orbital motion:

$$Vr = K[e\cos(\omega) + \cos(\theta + \omega)] + \gamma, \quad (1)$$

where K is the semi-amplitude of the RV variations, e is the eccentricity, ω is the position of the periastron, γ is the radial velocity of the center of gravity of the system, and θ is the true anomaly. A true anomaly can be decomposed in a series in degrees of eccentricity using the well-known formula:

$$\theta = M + 2e\sin(M) + 1.25e^2\sin(2M) - 4/3e^3\sin(M)[1 - 13/4\cos 2(M)] + ..., \quad (2)$$

where M = 2π ($\phi + \phi_0$) is the mean anomaly, ϕ is the phase of the orbital motion (ϕ [0,1]), and ϕ_0 is the phase shift between the theoretical and the observed RV curves, determined in the calculations. For small values of eccentricity, two or three first members of the decomposition are sufficient. The successful application of this method has been demonstrated, in particular, in the Pogodin et al. [31], [32].

The approximation of the observed and theoretical phase curve is carried out by minimizing the sum of squares of the residuals for different values of the orbital elements. When calculating each orbital parameter, the method of successive iterations was used; when the first values of all parameters, except one, are fixed, the value of which is determined at this stage. After that, the next parameter is selected and its value is specified. At each stage of the calculations, the fixed values for the remaining parameters are those that were counted in the previous stages. The process is repeated "in a circle" until convergence occurs, that is, when the sum of the squares of the residuals reaches a minimum. The final set of orbit parameters obtained by this procedure will be the solution. When: a) a small eccentricity and b) a successful choice of initial values of the determined parameters, convergence occurs fairly quickly (3 - 4 iteration cycles).

At the next step, the sum of the residuals is minimized for different values of the orbital period P, which allows it to be significantly clarified. As a result, we obtained a period of P = 3550 ± 28 days and a half-amplitude of the orbital velocity K = 28.8 ± 1.1 km/s. A theoretical orbital radial velocity curve for Vbis levels at 1.0Ic and 1.5Ic is shown in Fig.4 with a sinusoid curve. The observational data are best approximated by the theoretical radial velocity curve presented. For two values of the intensity level 1.0Ic and 1.5Ic, we obtained the system orbit elements, which are listed in Table 2 .

Table 2. Spectral orbit elements of the IL Cep A.

Orbital elements	1.0Ic	1.5 Ic	Mean
P_{orb} (days)	357	3530	3550 ± 28
γ(km/s)	28.0	29.6	28.8±1.1
K (km/s	-33.3	-27.5	-30.3 ± 4.1
e	0	0	0
$a_2 \sin i$ (au)			9.5
T_o=JD 2450000+	2921	2885	2903 ± 25

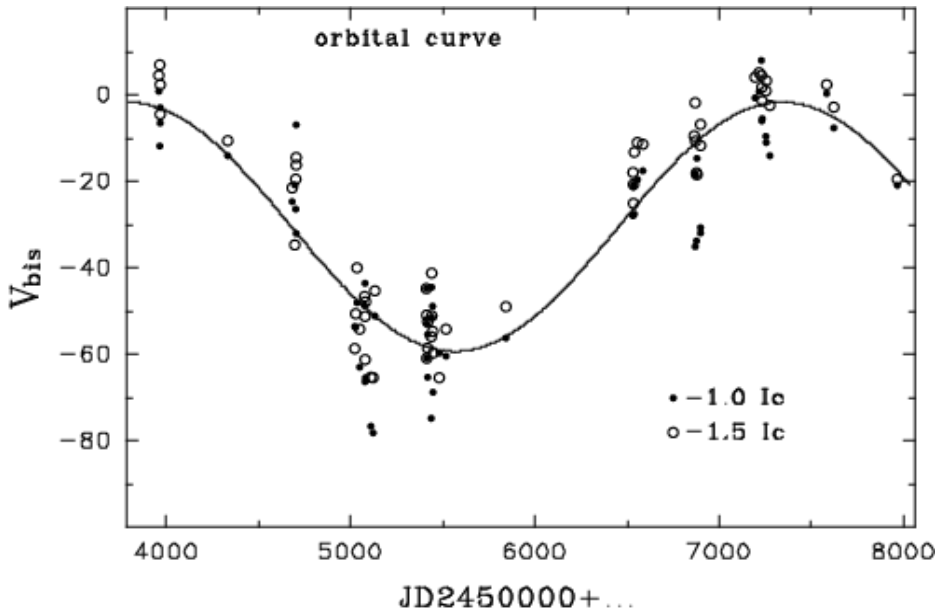

Fig. 4. Approximation of observational data using a theoretical radial-velocity curve for data from two different intensity levels, points — 1.0 I c and — 1.5 I c.

Here, P is the period, K is the semi-amplitude, γ is the radial velocity of the center of gravity of the system, e is the eccentricity, $a_2 \sin i$ is the major semi-orbital of the orbit, and To is the moment the curve passes through the gamma velocity. To estimate the masses of the components, you can use the standard equation for the mass function:

$$f(m) = \frac{K^3 P}{2\pi G} \tag{3}$$

accepting, sini = 1, and e = 0. Here K is the amplitude, P is the period, G is the gravitational constant. On the other hand, it is known that:

$$f_1 = (M) = \frac{M_2^3 \sin^3 i}{(M_1 + M_2)^2}, f_2(M) = \frac{M_1^3 \sin^3 i}{(M_1 + M_2)^2}. \quad (4)$$

For f (M), 8.7 M⊙ was obtained, which is in good agreement with the presented result for the mass function given in [19]. Then if we assume that the changes in RV relate to the shell of the main (massive) component of class B2, then the mass estimate for the second component M2, calculated from the following expression, is anomalously high:

$$M_2/M_\odot = 8.7(M_1/M_2 + 1)^2, \quad (5)$$

since M1/M2 $\geq$ 1. If the changes of K relate to the shell of the less massive component, then from the formula

$$M_1/M_\odot = 8.7(M_2/M_1 + 1)^2 \quad (6)$$

it follows that the mass of the main component cannot be less than 8.7M⊙. The typical mass for the B2 star is 10 M⊙ [33]. The mass of the second component is 0.7 M⊙. We can also estimate the distance between the components

$$a \sin i = \frac{KP}{2\pi}. \quad (7)$$

That is, even with sini = 1, the distance will be about 9.5 AU.

The assumption is that we can observe two shells - one for each of the components is not confirmed by observations. In this case, the half-width of the emission profile would have to change cyclically with a period equal to $R_{orb}/2$, but this is not observed. High amplitude variability of this magnitude is observed, but it is of a completely different nature and, apparently, is not associated with orbital motion.

The Hβ line shows two confidently separated emission components that are superimposed on broad photospheric wings. We also measured the RV of individual components of the Hβ emission line. Due to the lower level of the signal to the noise level of Hβ, measurement errors are about twice as bad as in the Hα line. Despite this, the average annual values of the bisector radial velocities of individual emission components of the Hβ line show a smooth multi-year synchronous change with the Hα line. The left panel of Fig.5 shows the time variation in the RV individual components of the Hβ line. As can be seen, the RV values of individual emission components practically are varied synchronously with the same amplitude. Therefore, the radial velocities for individual components in the

Hβ line show a high degree of correlation, r = 0.80 $\pm$ 0.086 (Fig. 5). Fig. 5 shows the relations of the radial velocities of the blue and red components of the Hβ emission. The correlation coefficient for Spearman has a 93% confidence. This observational is another argument is showing that the emission component arises as a result of the emission of the disk that belongs to only one of the components.

5. DISCUSSION AND CONCLUSIONS

So, spectral observations of the Be Herbig IL Cep A star of recent years have confirmed our assumption that the star is a spectral-binary system [19]. For the first time, we established a smooth variation in the radial velocities of the hydrogen emission lines Hα and Hβ. At the same time, the half-widths of Hα emission do not show periodic changes. This indicates that the observed emission is formed in the circumstellar disk, which belongs to only one of the components of the system. The synchronous displacement of individual components of the Hβ emission line, and the existence of the direct correlation of these components also confirms the assumption that the disk is only around one of the components of the system.

It was shown that the He I λ 5876 Åline has seasonal variations in radial velocities and equivalent widths that exceed measurement errors. However, these changes do not show a definite pattern. Lines D1, D2 NaI and DIB λ 5780, 5796 Åshowed a relatively high degree of stability. Small variations in the radial velocities of the D Na I lines shows that part of these lines are formed in the disk wind. Apparently, the values RV of these lines are corresponding to the velocity of the mass center of the system -11.8 $\pm$ 2.0 km/s. This also agrees well with the data of [10], for the interstellar line CaII, and with the data of [29].

Based on the above mentioned results, we have carried out the RV curves of system for the Hα emission line at different intensity levels. The most stable curves were obtained at the intensity level 1.0 Ic - 1.5 Ic of the spectral continuum. By using this method, we have determined the orbital elements of the system. An analysis of the obtained mass function of the system showed that if the mass of the primary component for a typical B2V star is 10 $M_{\odot}$, then the second component, which contains a disk emitting in emission lines, will have a mass of about 0.7 $M_{\odot}$.

The change for B-V occurs across all observations from 0.72 to 0.77 [34]. A similar value of the color index B-V for the IL Cep star is given in [21] and [16]. According to [35] and [21] for the complex Cep OB3, the extinction coefficient is R_V = 3.1 mag. If we assume that the brightest state of the B-V color corresponds to the brighter B2V component, then on the color index value for the main sequence stars $(B-V)_o$ = -0.22 [36] for the color excess we can get E(B-V) = +94. Then for the coefficient of reddening we get Av = 2.9 mag. For absolute and

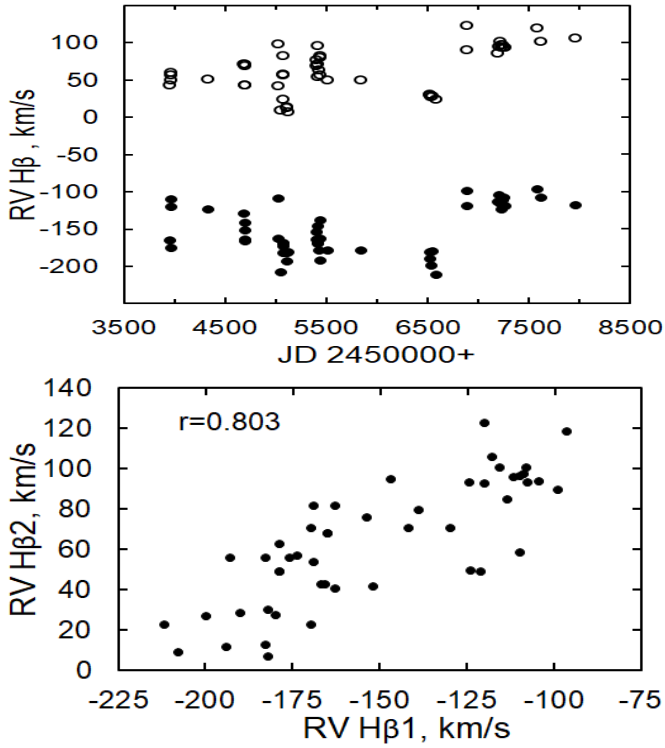

Fig. 5. Left panel: time variation in the bisector radial velocity of the emission components of the Hβ line. Dark circles, blue component, bright circles, red component. Right panel: the dependence of the radial velocities of the blue (RVHβ1) and red (RVHβ2) components.

bolometric luminosities, one can obtain $Mv = -2.9$, M_{bol} = - 5.25 and log $L/L\odot$ = 4.1. For the star B2V Te = 22000 K [36], then for the radius we get $logR/R\odot$ = 0.83. As we noted above, for the bright component, the mass should be about 10 $M_\odot$, and for the secondary component - 0.7 $M_\odot$. The secondary component of the system is rather a low-mass K4V star and has a long semi-transparent gas envelope. It must be said that, apparently, there are this type spectral-binary systems among the young stars. One of them is the well-known in Orion young θ1 Ori trapezium member system BM Ori [37].

Based on the results of this work, the following conclusions can be presented:

1. For the first time, the long-time periodic variability of the radial velocities of the hydrogen emission lines Hα and Hβ was established. The period of variability is P = 3550 $\pm$ 28 days and the spectroscopic elements of the orbit of the system are determined.

2. Equivalent widths and half widths of hydrogen lines show a certain variability, which does not occur synchronously with variations in the radial velocities of the emission component.

3. For the first time we have shown that the circumstellar disk, in which the emission spectrum is formed, belongs to only one of the components the low-mass component of the system.

4. Part of the D Na I lines can be formed in the stellar wind, the main part of these lines belongs to the interstellar medium.

This work was supported by the Science Development Foundation under the President of the Republic of Azerbaijan (grant Grant No EIF-BGM-4-RFTF-1/2017-21/07/1) as well as the Russian Foundation for Fundamental Research.

REFERENCES

1. Herbig, G.H. The Spectra of Be- and Ae-Type Stars Associated with Nebulosity. 1960, ApJS, 4, 337 [doi: 10.1086/190050]

2. The, P.S. de Winter D., Perez, M.R. A new catalogue of members and candidate members of the Herbig Ae/Be (HAEBE) stellar group. 1994, ApJS, 104, 315

3. Vieira, S.L.A., Corradi, W.J.B., Alencar, S.H.P., et al. Investigation of 131 Herbig Ae/Be Candidate Stars. 2003, AJ, 126, 2971 [doi: 10.1086/379553]

4. Grady, C.A., Woodgate, B.F., Bowers, C.W., et al. Coronagraphic Imaging of Pre-Main-Sequence Stars with the Hubble Space Telescope Space Telescope Imaging Spectrograph. I. The Herbig Ae Stars. 2005, ApJ, 630, 958 [doi: 10.1086/430731]

5. Fukagawa, M., Hayashi, M., Tamura, M., et al. Spiral Structure in the Circumstellar Disk around AB Aurigae. 2004, ApJ, 605, L53 [doi: 10.1086/420699]

6. Pirzkal, N., Spillar, E.J., Dyck, H.M. A Search for Close Bright Companions to AeBe Stars. 1997, ApJ, 481, 392 [doi: 10.1086/304055]

7. Wheelwright, H.E., Oudmaijer, R.D., Goodwin S.P. The mass ratio and formation mechanisms of Herbig Ae/Be star binary systems. 2010, MNRAS, 401, 1199 [doi: 10.1111/j.1365-2966.2009.15708.x]

8. Assousa, G.E., Herbst, W., Turner, K.C. Supernova-induced star formation in Cepheus OB3. 1977, ApJ, 218, L13 [doi: 10.1086/182566]

9. Peter, D., Feldt, M., Henning, Th., Hormuth, F. Massive binaries in the Cepheus OB2/3 region. Constraining the formation mechanism of massive stars. 2012, A&A, 538, A74 [doi: 10.1051/0004-6361/201015027]

10. Garmany, C.D. Internal motions in the association Cep OB3. 1973, AJ, 78, 185 [doi: 10.1086/111396]

11. Alesian, E., Wade, G.A., et al. A high-resolution spectropolarimetric survey of Herbig Ae/Be stars - II. Rotation. 2013, MNRAS, 429, 1001A [doi: 10.1093/mnras/sts384]

12. Crawford, D.L., Barnes, J.V. Standard stars for UVBY photometry. 1970, AJ, 75, 978 [doi: 10.1086/111051]

13. Hill, G. On Beta Cephei Stars: a Search for Beta Cephei Stars. 1967, ApJS, 14, 263 [doi: 10.1086/190156]

14. Samus, N.N., Durlevich, O.V., Kazarovets, E.V., et al. General Catalog of Variable Stars (GCVS database, Version 2012 Jan), CDS B/gcvs.

15. Hill, G., Hilditch, R.W., Pfannenschmidt E.L. Photoelectric measures of variable stars observed at Mt. Kobau. 1976, Publ. Dom. Astrophys. Observ., 15, 1

16. Mel'nikov S,Yu., Shevchenko, V.S., Grankin, K.N., Ibragimov, M.A., Yakubov, S.D. HD 216629=IL Cep, BHJ 71, and LkH alpha 350–Probable Herbig Ae/Be stars in the Cep OB3 association: HD 216629 AB and LkH alpha 350. 1996, Astron. Rep., 40, 350

17. Finkenzeller, U. Rotational velocities, spectral types, and forbidden lines of Herbig Ae/Be stars. 1985, A&A, 151, 340

18. Ismailov, N.Z., Bahaddinova, G.R., Kalilov, O.V., Mikailov, Kh.M. Spectral variability of IL cephei. 2013, ASTROPHYS BULL., 68, 2, 196

19. Ismailov, N.Z., Khalilov, O.V., Bakhaddinova, G.R. Optical spectrum variations of IL Cep A. 2016, Astron. Rep., 60, 2, 265 [doi: 10.1134/S1063772916020037]

20. Patel, P., Sigut, T.A.A., Landstreet, J.D. Photoionization Models for the Inner Gaseous Disks of Herbig Be Stars: Evidence against Magnetospheric. Accretion. 2017, ApJ, 836, 214, 20 [doi: 10.3847/1538-4357/aa5c3f]

21. Finkenzeller, U., Mundt, R. The Herbig Ae/Be stars associated with nebulosity. 1984, A&AS, 55, 109

22. Acke, B., van den Ancker, M.E., Dullemond, C.P. [O I] 6300 Å emission in Herbig Ae/Be systems: Signature of Keplerian rotation. 2005, A&A, 436, 209 [doi: 10.1051/0004-6361:20042484]

23. Grinin, V., Tambovtseva, L., Potravnov, I., Mkrtichian, D. Disk Wind in the Radiation of Two Herbig Ae/Be Stars: MWC 480 and IL Cep. 2017, ASP Conference Series, 508, 185

24. Mikailov, Kh.M., Khalilov, V.M., Alekberov, I.A. Spectral investigations of the symbiotic star CH Cygni. 2005, Tsirk. ShAO, 109, 21

25. Галазутдинов, Г.А. 1992, Препринт САО РАН, 92

26. Mikayilov, Kh.M., Musayev, F.A., Alakbarov, I.A., et al., SHaFES: Shamakhy Fibre Echelle Spectrograph, 2017, AJA, 12, 1, 4

27. Boehm, T., Catala, C. Rotation, winds and active phenomena in Herbig Ae/Be stars. 1995, A&A, 301, 155

28. Ismailov, N.Z., Khalilov, O.V., Bahaddinova, G.R. HeI 5876 Line Structure in the Spectra of IL CEP a. 2015, Odessa Astron. Pub., 28, 231

29. Tie Liu, Huawei Zhang, Yuefang Wu, Sheng-Li Qin, & Martin Miller. Evolution of the dust/gas environment around Herbig Ae/Be stars. 2011, ApJ, 734:22 (16pp) [doi: 10.1088/0004-637X/734/1/22]

30. Pogodin, M.A., et al. A new phase of activity of the Herbig Be star HD 200775 in 2001: Evidence for binarity. 2004, A&A, 417, 715 [doi: 10.1051/0004-6361:20031783]

31. Pogodin, M.A., Drake, N.A., Jilinski, E.G., Pereira, C.B., The unusual binary HD 83058 in the region of the Scorpius-Centaurus OB association. 2014, Proc. Symp. IAU, 302, 315 [doi: 10.1017/S1743921314002397]

32. Pogodin, M. A., Drake, N. A., Jilinski, E. G. The Unusual Binary System HD83058 in the OB Association Sco-Cen, 2019, Astrophysica 62, 183

33. Straizys, V.,Kuriliene, G. Fundamental stellar parameters derived from the evolutionary tracks. 1981, Ap&SS, 80, 353 [doi: 10.1007/BF00652936]

34. Herbst, W., Herbst, D.K., Grossman E.J., et al. Catalogue of UBVRI photometry of T Tauri stars and analysis of the causes of their variability. 1994, AJ, 108, 1906 [doi: 10.1086/117204]

35. Garrison, R.F. Spectral classification in the association III Cephei and the ratio of total-to-selective absorption. 1970, AJ, 75, 1001 [doi: 10.1086/111053]

36. Kenyon, S.J., Hartmann, L. Pre-Main-Sequence Evolution in the Taurus-Auriga Molecular Cloud. 1995, ApJS, 101, 117 [doi: 10.1086/192235]

37. Antokhina, E.A., Ismailov, N.Z., Cherepashchuk, A.M. The parameters of the eclipsed binary system BM ORI - A member of Theta 1 ORI trapezium. 1989, Sov. Astron. Lett., 15, 362

İL CEP ULDUZUNUN ÇOXİLLİK SPEKTRAL MÜŞAHİDƏLƏRİNİN NƏTİCƏLƏRİ

***N. Z. İsmayılov*[a], *M. A. Poqodin*[b], *Ü. Z. Bəşirova*[a], *G. R. Bahəddinova*[a]**

[a] *N.Tusi adına Şamaxı Astrofizika Rəsədxanası, Azərbaycan Milli Elmlər Akademiyası, Şamaxı rayonu, Azərbaycan*
[b] *Pulkova Astrofizika Rəsədxanası, Rusiya Elmlər Akademiyası, Sankt-Peterburq, Rusiya*

Be Herbiq tipli İL Cep ulduzunun çoxillik spectral müşahidələrinin nəticələri verilmişdir. İlk dəfə, hidrogenin Hα və Hβ xətlərinin şüalanma komponentlərinin şüa sürətlərinin hamar əyri boyunca dəyişməsi aşkar edilmişdir. D Na I və DIB λ5780, 5796Å xətlərinin şüa sürətləri ulduzlararası mühitin şüa sürətinə uyğun gəlir. Göstərilmişdir ki, hidrogenin şüalanma xəttləri çox güman ki, yalnız qoşa sistemin komponentlərindən biri ətrafında formalaşmışdır. Sistemin orbit elementləri periodu 3550$\pm$28 gün olan spectral qoşa ulduz modelində təyin edilmişdir. Komponentlərin mümkün fundamental parametrləri təyin edilmişdir. Güman olunur ki, sistemin ikinci komponenti ətrafında disk olan cavan ulduzdur.

Açar sözlər: Ulduzlar – Cavan qoşa ulduzlar – Ae/Be Herbiq tipli ulduzlar – Spectral dəyişkənlik – İL Cep A

STUDY OF PHOTOMETRIC VARIABILITY OF MAGNETIC CP STARS II.NATURE OF BRIGHTNESS VARIATION

S. G. Aliyev [*] **, *V. M. Khalilov*, *Z. M. Alishova***

Shamakhy Astrophysical Observatory named after N.Tusi,
Azerbaijan National Academy of Sciences, Shamakhy region, Azerbaijan

Phase light curves have been build based on photometric materials, obtained in 10 colors for different (B0-F0) magnetic CP stars. The light curves observed in the form of a double wave for most stars. The changes in the light curves occur in counter-phase, in different bands for some of the investigated late CP stars (A2-F0) of the SrCrEu type. It is shown, that the brightness variability in antiphase is explained by the energy blocking in the region $\lambda\lambda$5000 - 5500 ÅÅ(in range of depression λ5200Å), created mainly by rare earth elements, the excesses are reaching in the atmosphere of these stars 4.0 - 6.0 dex.

Keywords: magnetic stars– photometric variability.

1. INTRODUCTION

Firmly established, that magnetic chemically peculiar (MCP) stars are part of a more general class of chemically peculiar (CP) main sequence stars, located in the spectral range B0 - F0. The abnormally strong lines of a large set of chemical elements (Si, Cr, Sr, Mn, Eu, etc) and the presence of a powerful magnetic field and relatively low-velocity axial rotation ($V \sin I \leq 60$ km s^{-1}) compared to with normal stars ($V \sin i = 170$ km s^{-1}) are the general property of these stars. According to the classification [1], [2], magnetic CP stars divided into five main groups: λ5200- Si, Si, Si-Cr-Eu, Sr-Cr-Eu and Sr. This sequence is statistically correlated with the color indices and consequently, with the effective temperature [2]. The photometric classification of MCP stars based on measurements of the magnitude, of the anomalies in the energy distribution in the continuous spectrum.

[*] E-mail: sabirshao5@gmail.com

According to [3], in various photometric systems, these stars are standing out differently. Photometrical variability, as well as spectral and magnetic variability, is a characteristic property for all magnetic CP stars. Gutnik [4] observed periodic changes in the brightness of magnetic CP - stars HD 112185 (ϵ UMa) and HD 112413 (α2 CVn) in 1917. Intensive studies of the photometric variability of these stars began [5–7]and others after the discovery of the strong magnetic field (Be $\approx 10^2 - 10^4$G), of these stars by Babcock. The amplitude of photometrical changes is small, in visual rays; it is $0^m.01$–$0^m.04$ stellar magnitude. Simultaneously with brightness variation occurs variation of color. Intensive studies of the photometric variability of these stars began after the discovery by Babcock a strong magnetic field of these stars (Be $\approx 10^2 - 10^4$ G) [5–7] and others. Variation of color of the star can be both in phase and in antiphase with brightness variation. The light curves of some stars change in antiphase not only with magnetic and spectral changes but also with show changes in different rays (bands) between themselves. There are cases when a double wave is observed in one band, one wave in another, either weak changes or their absence in another band. The ambiguity in the action of the color and brightness of these stars did not allow finding simple explanations of these phenomena. Naturally, it can be assumed that the photometric conduct of MCP stars related to the peculiarity effect. This paper is devoted mainly to the study of a possible connection between the photometric conduct and the peculiarity effect for magnetic CP stars.

Periodic brightness variations observed of all known magnetic CP stars. At present time, accepted that variations of the brightness associated with non-uniform distribution of the chemical anomaly in the atmospheres of these stars. The photometric variability of MCP stars was studied not only with the help of broadband UVB and similar systems but also, with widespread observations in different narrow-band systems, particularly, a 10-colour system [7].The investigations in the narrow-band system, allow us to determine the observed various small photometric effects (wide and small anomalies in the continuum - depressions, see below) observed in these stars.

In this study, have been made attempts to find the reason for the different character of the brightness variability of magnetic CP stars using observational materials obtained in a 10-colour photometric system.

2. OBSERVATIONS AND PROCESSING.

In order to identify the various type of the photometric variability of MCP stars, at the Shamakhy Astrophysical Observatory were used homogeneous ten colored photometric observational materials, which were obtained using a 40 cm telescope of observing station of the Central Aerial Research Institute of the GDR.

Further observations carried out on a dual photometric telescope manufactured at the Central Aerial Research Institute of the GDR [8], for increasing the data accuracy obtained during photometric investigations of variable stars, which allows obtaining data on the studied star and the comparison star, simultaneously. The observations were carried out in 10-colours: U- λ3450Å, P -λ3740Å, X - λ4050Å, Y- λ4660 Å, Z - λ5160Å, V- λ5450Å, HR- λ6150Å, S- λ6550Å, MR- λ7200Å, DR- λ7650Å covering the wavelength range from 3400 Å to 8000 Å. Seven of these filters are identical with Vilnius photometric system filters [9]. The remaining three glass filter combinations (S, MR and DR) chosen to cover the long-wavelength part of the spectrum ($\lambda\lambda$6470 - 8000Å).

Observational materials, both photometric and spectral, conducted at the 2-m telescope of the Shamakhy Astrophysical Observatory of the Academy of Sciences of Azerbaijan, were obtained almost simultaneously (or in one season). Information about the spectral materials and their quality, presented in the conference materials on magnetic stars [10]. Spectrograms used to determine the effective temperature and Vsini velocities for most studied stars, which shown in tables 1 - 4. The obtained photometrical materials are homogeneous, high precision ($0^m.005$–$0^m.007$) and available for detecting wide and small anomalies (depressions) of the continuum, in the range λ4200, λ5200 and λ6300 Å, which are typical for MCP stars. Therefore, the 10-colour photometric system is very useful for both the photometric extraction of MCP stars and the investigation of the character of the photometric variability of these stars.

More than 30 stars included in the observation program. The periods (P) of some stars were refined using the obtained materials. The final values of the magnitudes (P) given in the fifth column of table 1. General information for the investigated MCP stars given in table 1, in columns of which the following data are successively shown: 1 is the number of stars on HD, 2 is stellar magnitude, 3-spectral class (SP), 4 is the peculiarity type, 5 is the rotation period P (d) in days, 6 is the effective temperature (mainly taken from [11], [12] and other sources, 7 is the projection of the velocity of rotation of a star to the line of vision - V Sin I (in km s^{-1}) - taken from [13], [14] and one of the authors of this work (Aliyev [15]); 8 is the root-mean-square magnitude of the longitudinal magnetic field (Be) taken from the work Romanyuk et al. [16]; 9 - index Vienna system is - $\Delta\alpha$, 10 – index Geneva system is- Z (in stellar magnitudes). The magnitudes Z and $\Delta\alpha$ taken from [16] and other resources. Both parameters allow you to determine the magnitude of the depression at 5200Å. Wide depressions in the energy distribution curves of MCP stars, around λ 5200Å detected by Wolf [17]. Further, was discovered that in the temperature interval from 8000 K to 14000 K observing very wide (200–400 Å) and shallow (several percent's) depression in the continuum in magnetic CP stars [16], [18].

Table 1. MCP stars

HD	mv	Sp	Pecul.	P(d)	Te	Vsini	Be(G)	$\Delta\alpha$	Z
4778	6.15	A2	SrCrEu	2.562	8500	–	1030	-	-0.045
15089	4.59	A4	SrCr	1.740	8400	47	203	small	Small
19832	5.65	B7	HeSi	0.728	12390	200	360	0.015	-0.020
25354	7.9	A0	SrCrEu	3.901	9000	–	206	small	-0.025
25823	5.27	B7	SrSi	7.227	13000	16	868	0.032	-0.030
27309	5.38	A0	Si	1.569	11820	66	1755	0.065	-0.059
34452	5.39	B4	SiHe	2.466	14110	62	743	0.061	-0.056
40312	2.64	B9	SiCr	3.619	10100	48	340	0.028	-0.019
51418	6.6	A1	SrCrEu	5.4	9500	–	400	0.032	-0.042
65339	6.00	A2	SrCrEu	8.027	10000	15	1200	-	-
71866	6.75	A5	SiSrEu	6.800	8650	20	1680	0.056	-0.058
74521	5.65	A1	SiCrEu	5.43	10600	20	812	0.076	-0.061
108662	5.25	A0	SrCrEu	5.07	9900	18	620	0.050	-0.040
108945	5.49	A2	SrEu	2.004	8950	66	537	0.026	-0.027
112185	1.68	A1	CrCa	5.089	9800	25	600	-	-
112413	2.90	A0	SiCrEu	5.469	11180	24	1350	0.040	-0.032
118022	4.93	A2	SrCrEu	3.722	9050	10	808	0.050	-0.052
119213	6.3	A2	SrCrEu	2.450	9800	25	1220	0.026	-0.031
124224	4.90	A0	SiCrHe	0.521	12460	120	570	0.020	-0.020
133029	6.16	B9	SiCrSr	2.89	10520	20	2420	0.064	-0.059
137909	3.72	A9	SrCrEu	18.487	7400	18	280	-	-
140160	5.26	A0	SiSrCr	1.596	9150	66	860	0.028	-0.024
153882	6.29	B9	SrCrEu	6.009	8900	20	1750	0.049	-0.046
173650	6.39	B9	SiSrCr	9.975	8950	22	326	0.020	-0.030
184905	6.62	A0	CrSiEu	1.845	10800	–	+3000	-	-0.023
188041	5.6	A5	SrCrEu	224 0.933	8000	21	1100	0.075	-0.059
192913	6.7	A0	SiCr	16.8	10600	–	483	0.048	-0.034
193722	6.2	B8	SiSrEu	1.133	11600	47	–	0.046	-0.025
196502	5.2	A2	SrCrEu	20.27	8700	10	490	0.072	-0.043
215441	8.84	A0	Si	9.48	15900	–	17500	–	-0.056
220825	4.94	B9	CrSr	0.583	9700	34	270	0.034	-0.033
221568	8.0	A2	SrCrEu	160	9000	15	1800	–	–
224801	6.40	B8	SiSrEu	3.740	11800	37	+2300	0.055	-0.032

Further, was discovered that in the temperature interval from 8000 K to 14000 K observing very wide (200–400 Å) and shallow (several percent's) depression in

the continuum in magnetic CP stars [16], [18]. Outside of this temperature interval, depressions have not observed. Their maximum magnitude is reaching at CP stars, located in the spectral interval B9-A2. Such weak anomalies of the continuum could not be determined earlier, according to photographic registrations of astronomical observations. They were discovered after using photoelectric registering methods of observations, including a 10-colour photometric system.

The 10-colour systems, [8] contain filters, which have bandwidth located in optimal places for measuring areas of increased blocking (range of depression) and the altitude of the Balmer jump. The altitude of discontinuity given by indices the U-X or U-Y and the blockings around λ5200 Åare indices Y-Z or Z-S. The filter band pass of the 10-colour system (λ = 5160 Å) is exclusively useful for detecting a region of increased blocking (λ = 5200 Å) and thus detecting chemically peculiar stars. The results of investigations in the 10-colour system, which began in 1970 by Schöneich [19–21], can significantly facilitate the interpretation of complex phenomena, occurring in atmospheres of exclusively interesting and numerous MCP stars. Based on these materials, we constructed phase light curves in all colors (filters) for most of the studied stars presented in Table 1.

3. ANALYSIS OF LIGHT CURVES

Constructed phase light curves, have a different character depending on the type of peculiarity, the intensity of the magnetic field, the effective temperature and other characteristics of the investigated stars. As a result of the analysis, was identified, that based on the nature of the brightness variation with the wavelength (in different bands), all the observed phase curve dependences for the studied stars can be classified into three groups.

As an example, figures 1-3 show the phase light curves from each group of investigated stars with different characteristics (see Tables 2, 3 and 4).

The first one of this contains those stars, for which the light curves in the entire observable region (λ3400 - 8000 ÅÅ) change in phase and with close amplitude (Fig.1).

The second group includes stars that the brightness in different colors changing significantly and in the (depression) region $\lambda\lambda$5000 - 5500 Ådecreases to the minimum value (Fig. 2).

The third group includes those stars, that the brightness variation in the short region (λ <5000Å) and in the long-wave regions (λ> 5500 Å) of the spectrum, occurs in a antiphase (Fig. 3).

Tables 1, 3, and 4 show the stars that belong to the first, second, and third groups, respectively. The designation is the same as in table.1.

All the stars of the first group are hot (helium and silicic) stars that have temperatures above 10000K. Most of the energy in the spectrum of these stars radiated in the ultraviolet (UV). The blocked energy by the lines of the continuous spectrum in the UV region re-radiated in a longer wave. Wherein this backwarming effect occurs. Preston has noted [22], that the reradiating of blocked energy from the ultraviolet to the visible portion of the spectrum can play significant role in explaining the photometric behavior of these stars. Further, this problem studied by Mushielok [23], where the results of the record of the transfer of blocked energy from the ultraviolet to the visible region of the spectrum, which allows explaining the observed change in brightness with wavelength, presented.

Special interest is the extra-atmospheric observations of Molnar [24], in which was obtained, that changes in the radiation of far ultraviolet occur in antiphase, with changes in the visible region of the spectrum. This is powerful argument for support of the existence of processes of transferring blocked energy from the ultraviolet to the visible region of the spectrum (backwarming effect). We join the opinion of Preston and Mushek, to explain the photometric behavior of the first group of the stars based on these facts. The brightness in all bands for these stars changes close by the magnitude of amplitude, because of change in the colour indices of these stars does not occur, as is typical for stars of this group. Thus, the effect of blocking and transferring energy from the UV region of the spectrum sufficiently describes the observable brightness variation with wavelength for the first group of stars.

The amplitudes of variations in different bands, change significantly and in Z (5160 Å) and V (5420Å) bands, the variability decreases in comparison with the neighboring bands for the second group of stars. Apparently, this connected to the fact, that decrease in brightness occurs because of an increase in blocking in the ultraviolet region, while in the same time an increase in brightness occurs in the visible region of the spectrum due to the retro-thermal effect (backwarming effect). Both effects counteract each other and, respectively, the variability for these stars (Table 3) reaches the minimum (up to the threshold of measurement sensitivity of the device).

It should be added that for most magnetic CP stars, due to the peculiarity effect, extra continuous absorption bands of depression arises in the spotted regions on the wave-length $\lambda\lambda$5000-5400ÅÅ. According to [16], [25], the main contribution to the depression on λ5200Å made by the FeI lines and the low-activated FeII lines. According to [26], the depressions on λ5200Å run high with an increase in the magnitude of the magnetic field and the metal content in the stellar atmosphere. As is known [26], the maximum depressions in the continuum detected mainly in the second group of stars. The basic causes of the photometrical behavior for the second group of stars are the blocking and back-warming effect and the

appearance and amplification of the depression (in the region $\lambda\lambda$5000-5400ÅÅ) due to the magnetic field.

The brightness amplitude decreasing in the Z and V bands (in the depression region), which located in the A2 - F0 spectral range, is also observed in the third group of MCP stars. The amplitude of the variability of this group of stars, in different rays, changes significantly and decreases significantly in the region of the Z and V bands (5000 - 5500 Å), that are brightness variation is not observed. Generally, in the literature, such wavelength regions named the null wavelength region. Unlike the second group, the brightness for this group of stars in the short (λ <5000 Å) and long-wave (5500-8000 Å) spectral regions changes in antiphase. As an example, Fig. 3 shows the light curves for the star HD119213. A similar picture observed in other cool MCP stars, which belong to the peculiarity type SrCrEu (see Table 4), that is, all these stars are rare-earth stars.

Comparison of the built-up phase dependences of the investigated stars shows that the highest variability is detecting in cool (A2-F0) stars, which are (SrCrEu) stars. Analogous results have obtained as early as 1973 by Kodaira [27], where some spectral and photometric data collected for 49 magnetic stars. It had found that comparatively high variations show stars, which have strong lines of Eu and other lanthanides. In works [24], [28] had obtained that a strong blocking by lines of rare - earth elements in the UV region of around 1600 Å, resulting in the redistribution of energy in the visual region of the spectrum.

Table 2. The main parameters of some stars of the third group (*Light curves changes in antiphase*).

HD	**mv**	**SP**	**Pecul.**	**P(d)**	**v sini km s^{-1}**	**Be (G)**	$\Delta\alpha$	**Z**	Δm_v
19832	5.65	B7	He Si	0.73	136	315	0.015	-0.020	0.040
27309	5.38	A1	Si	1.57	44	1755	0.065	-0.059	0.030
140160	5.26	A0	SrCr	1.6	50	860	0.028	-0.024	0.020
173650	6.39	B9	SiSrCr	9.98	18	326	0.020	-0.030	0.045
184905	6.62	A0	SiCrSr	1.84	18	3000	0.032	-0.023	0.042
215441	8.84	A0	Si	9.48	15	17500	-	-0.056	0.110

If we take into account that the photometric variability of magnetic CP stars is mainly caused by the blanketing effect, which occurs by the combination of lines of all peculiar elements, then indicated above facts allow us to conclude that for rare-earth stars, the main role in the brightness variations and color index plays lanthanides excess (more than 5-dex). There are enough indications [27],

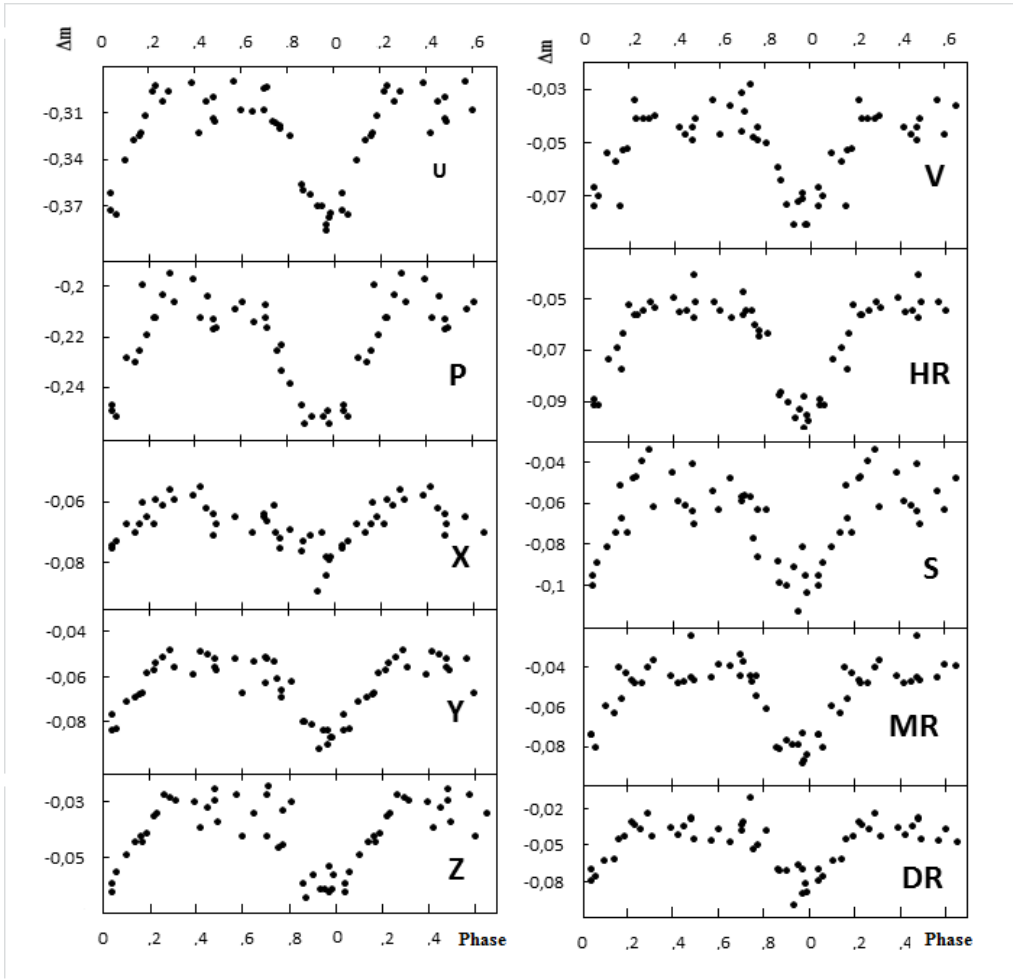

Fig. 1. The light curves of the star HD 184905.

[29] that SrCrEu type of the MCP stars have very strong lines of europium and other lanthanides (for example, Ce, Nd, Sm, Gd), which are associated by their overabundance in the atmospheres of these stars.

In works [29], [30] had obtained that in the atmospheres of MCP stars, the excess of rare-earth elements is reaching 5 - 6dex. Based on the above facts it can be concluded, that the brightness variation in counter-phase, in different rays of the third group of stars, is due to the fact, that continuous absorption occurs in the visible region, (including the depression region λ5200Å) - blanketing by lines of rare-earth elements, without causing UV absorption and back-warming effect in the visible region of the spectrum. In addition, the magnetic field, which is typical for these stars, leads to increased blanketing and redistribution of energy

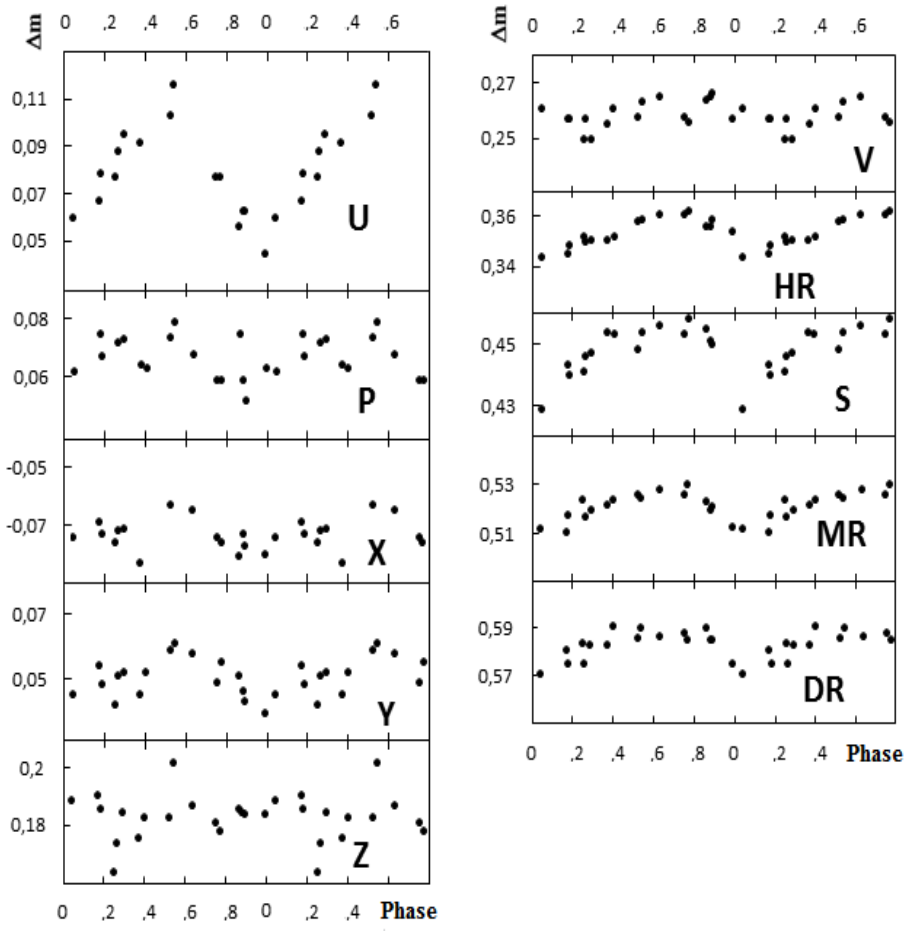

Fig. 2. Light curves of star HD 65339 (53 Cam).

Table 3. The main parameters of some stars of the second group. (Light curves in the (depression) region ($\lambda\lambda$5000 - 5500 ÅÅ) decreases to the minimum value)

HD	m_v	SP	Pecul.	P(d)	v sini km s^{-1}	Be(G)	$\Delta\alpha$	Z	Δm_v
65339	6.0	A2	SrCrEu	8.03	15	3200	0.03	-	0.012
112185	1.68	A1	CrCa.	5.09	20	800	0.06	-0.054	0.024
112413	2.90	A0	SrCrEu	5.47	18	1500	-	-0.033	0.030
219749	6.3	B 9	Si, P	1.62	74	-310	0.03	-	0.015

in the star's spectrum, resulting in anomalies in the continuum [31], that is, the magnetic field is increasing magnetic line blanketing and depression in the continuum. According to Vytautas Straižys [32], absorbed energy in a star's atmosphere re-emitted on longer wavelengths, causing a back-warming effect. This means that the blocked energy in the visible region, including the region of depression could re-emitted in the long-wavelength ($\lambda >$ 10,000 Å red) of spectrum region.

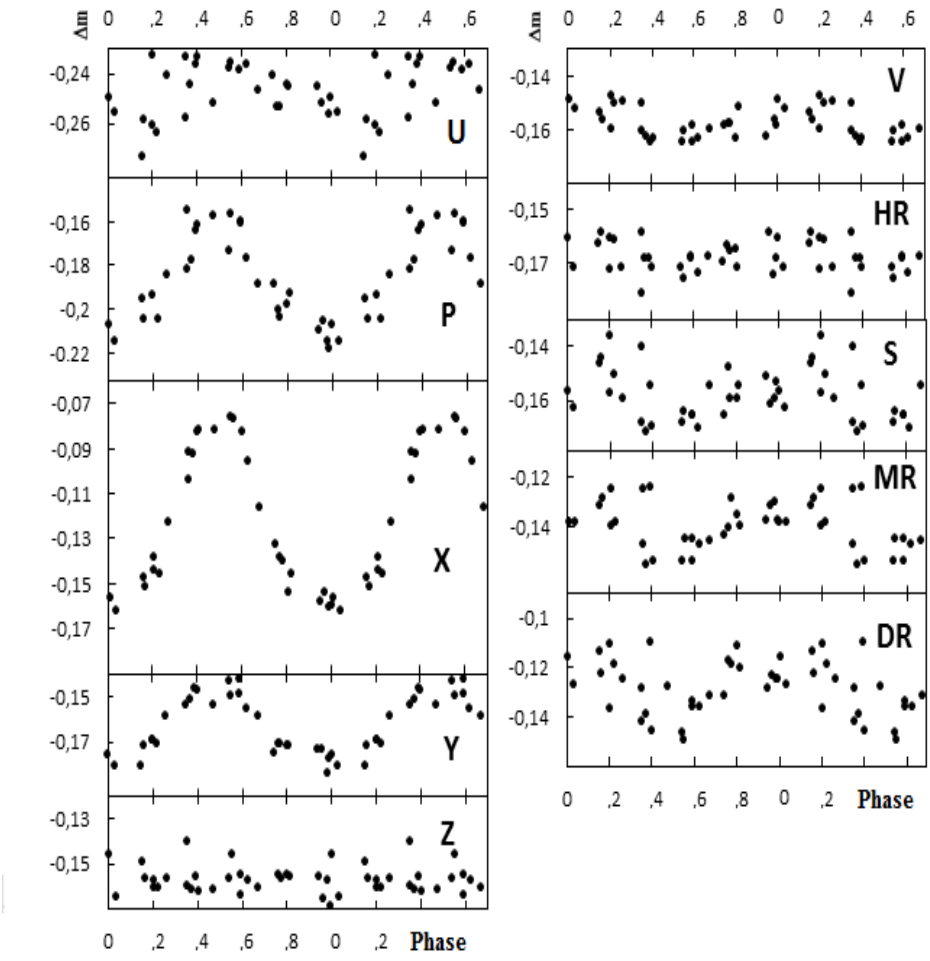

Fig. 3. Light curves of star H D119213

Therefore the decrease in brightness due to blocking by the REE lines in the range of depression, cannot be accompanied by an increase in brightness due to the back-warming effect in the visible ($\lambda <$8000Å) region of the spectrum.

Thus, the blocking of energy by the lines of rare-earth elements in the visible region and on the range of depression, leads to the cooling of the atmosphere, as

Table 4. The main parameters of some stars of the third group

(*Light curves changes in antiphase*).

HD	m_v	SP	Pecul.	P(d)	Vsini km s^{-1}	Be (G)	$\Delta\alpha$	Z	Δm_v
4778	6.15	A2	SrCrEu	2.56	33	1030	-	-0.045	0.020
119213	6.3	A2	SrCrEu	2.44	18	1220	0.026	-0.031	0.014
188041	5.6	F0	SrCrEu	224	20	1100	0.090	-0.059	0.015
196502	5.2	A2	SrCrEu	20.2	10	490	0.072	-0.043	0.030
221568	8.0	A2	SrCrEu	160	-	1800	-	-	0.012

a result of the brightness decreases in the upper layers of the atmosphere ($\lambda>$ 5500Å). As a result, in the spectral region $\lambda <$5000 Åand $\lambda>$ 5500Å, the brightness variation occurs in counter-phase, for the third group of stars. The blocked energy by the REE lines in the visible region, including in the Z and V bands, (range of depression), is reemitted in the long-wavelength ($\lambda>$ 10,000 Å) region of the spectrum.

Exoatmospheric observations of Molnar [24] and Jeimer (Aliev [33] and citations therein) shows that changes of the stream in the ultraviolet region, occur in counter-phase with variations in the stream in the visible region of the spectrum. This is a strong argument for the existence of processes of transfer of blocked energy from the ultraviolet region to the visible region of the spectrum (back-warming effect). Seemingly, the existence of processes of this type are the primary causes for the observed brightness variations for hot silicon MCP stars. However, it is necessary to take into account the magnetic line blanketing effect [30].

However, the photometric behaviors of other types of magnetic stars cannot explained only by the back-warming effect, which can lead to an overall temperature increase without causing a noticeable change in the structure of the star's atmosphere. To interpret the photometric behavior of the investigated stars, it is necessary, to take into account the influence of the magnetic field on the structure of the star's atmosphere.

4. DISCUSSION AND CONCLUSIONS.

Many works [7], [17], [23], [27], [33] have devoted to interpreting the nature of the observable brightness variations and color of MCP stars. In the study of Khokhlova [34], the following reasons examined in detail which can lead to a

change in the brightness and color of magnetic CP stars: a) a change in spectral line intensity of anomalously abundant elements; b) temperature non-uniformity; c) the non-sphericity of the figure of magnetic CP stars. She noted that the listed mechanisms do not allow fully explaining the observable specificities of changes in the brightness and color at these stars.

The magnitude of the brightness variability in the wavelength region $\lambda\lambda$5000 - 5500Åis very small or almost absent, for stars that presented in Tables 3 and 4. More interesting is the fact that for late (A2 - F0) rare earth (third group) stars, the light curves are in counter-phase in different bands (Fig. 3). Such a diverse nature of the brightness variability of magnetic CP stars is observed not only in narrow-band but also in broadband systems UVB and UVBY (for example, in magnetic CP-stars HD 4778 and HD 221568) [18]. The brightness in these stars changes in counter-phase in different bands (V and B) and (v and y). Such behavior of the brightness, especially, brightness variation in counter-phase, was not explained and interpreted by anyone yet.

Brightness variation in counter-phase in different rays of the third group of stars, as indicated above, is due to continuous absorption (blanketing) by REE lines in the visible region, including the range of depression (λ5200Å). Besides, the magnetic field increases magnetic line blanketing and leads to the emergence and amplification of depression in the continuum [31]. Because of blocking of energy in the visible region including the region of depression by the REE lines occurs cooling in the upper atmosphere, which causes a decrease in brightness in the upper layers ($\lambda >$ 5500Å) of the atmosphere. The brightness decrease is not accompanied to its increase due to the back-warming effect for these stars. As a result, in the spectral region $\lambda <$5000 Åand $\lambda >$ 5500Å, the brightness variation occurs in counter-phase for the third group of (rare-earth) stars. According to [32] the energy blocked by REE lines in the visible region of the spectrum, including in the range of depression of λ5200 Å could re-emitted in the long-wave spectral region ($\lambda >$ 10,000 Å), without causing back-warming effect in the visible spectral region.

An analysis of the light curves for the second and third groups of stars shows that the magnitude of the brightness variability in the wavelength region $\lambda\lambda$5000 - 5500Å is very small or almost absent, i.e. in this band ($\Delta\lambda$ = 5000Å), the brightness variations do not occur in fact. The average value of the wave-length - λ0 for this band usually called the null wavelength regions [33], [35]. The brightness variations at λ (5000Å) $<\lambda$0 occur in counter-phase with changes at λ (5500Å)$>$ λ0 for the third group of stars. The null wavelength region for these stars corresponds to λ0 = 5250Å(average value) and for the stars HD 4778 and HD 221568 - λ0 = 4600Å(v band).

Similar results obtained in the work of Sokolov [35], where used extra-atmospheric observations were carried out from the Hipparcos satellite. It also obtained that for the first group of magnetic stars CU Vir and 56 Ari null wavelength regions are located at $\lambda 0$ = 1213Å, and for the silicon star, HD112413 $\lambda 0$ = 2900Å. Details on the basic features of null wavelengths will be present in the subsequent works.

The preliminary results of this study presented in work [36], where features of the photometric behavior for different magnetic CP stars, most of which included in Table 1.

Main conclusions

1. The brightness of the early (B8-B0) MCP stars in the whole observable region, change in phase with close in the magnitude of amplitude, which associated with the transfer of blocked energy from the ultraviolet region to the visible range of the spectrum.

2. The brightness amplitudes for the second group of the investigated stars change in different rays significantly and in the region $\lambda\lambda$, 5000–5500Å decreases to the minimum value. This is explaining by the occurring of depression in the continuum at the atmosphere of these stars.

3. It was obtained that the brightness variation in counter-phase for magnetic A2-F0 stars is due to the blocking of lanthanide lines in the visible range of the continuum, particularly in the range of depression (λ5200 Å).

REFERENCES

1. Osawa, K. Specktral classification and three-color photometry of A-type peculiar stars. 1965, Ann.Tokio Astron.Obs., 2, 9, 123

2. Jaschek, M., Jaschek, C. The position of peculiar A-type stars in the color- absolute magnitude diagram. 1958, Z. fur Astrophys., 45, 35

3. Faraggiana, R. Recent progress in CP star detection and classification. 1987, Ap&SS, 134, 381

4. Gutnik, P. Übersicht über die Ergebnisse lichtelektrischer Messungen. 1917, Astron. Nachr., 205, 97

5. Jarzembowski, T. Light curve of magnetic star HD 215441 and variables. 1960, Acta Astron., 10, 4, 31

6. Preston, G., Stepin, K. The light, magnetic and radial velocity variations of HD10783. 1968, ApJ, 154, 971

7. Николов, А., Шенайх, В. Фотометрические исследования магнитных Ap-звезд, Сб. Магнитные Ap- звезды, под ред. Асланова И.А., изд. «Элм», 1975, 27

8. Хубрик, Х. Ю.,Шенайх, В. Двойной фотометрический телескоп в ШАО НАНА. Магнитные Ap- звезды. l975, с.157-159.

9. Страйжис, В. Многоцветная фотометрия звезд. г. Вильнюс, изд. «Мокслакс», 1977, 305

10. Сборник Магнитные Ap-звезды. под ред. Асланова И.А., изд. «Элм», 1975, 38

11. Алиев, С.Г. Определение эффективных температур магнитных звезд с учетом неоднородности атмосферы магнитных звезд. 2010, Transactions of National Academy of Sciences of Azerbaijan, XXXV, 2, 173

12. Glagolevskij, Yu. V. A new list effective temperature of chemically peculiar stars. 2002, Bull. Spec. Astrophys. Obs. 53, 33

13. Abt, H.A. Are stellar rotational axes distributed randomly. 2001, AJ, 122, 2008

14. Wolff, S.C. The rotation velocities' of magnetic Ap-stars. 1981, ApJ, 244, 221

15. Алиев, С.Г. Определение и анализ вращения магнитных и нормальных везд спектрального класса B0-F0 расположенные на ГП. 2016, Известия НАНА, Серия Физика и Астрономия, 36, 2,161

16. Романюк, И.И., Кудрявцев, Д.О., Семенко Е.А. Магнитные поля химически пекулярных звузд. II. 2009, Астрофизический бюллетень, 64, 3, 247

17. Wolff, S.C. A Spectroscopic and Photometric Study of the Ap Stars. 1967, ApJS, 15, 21

18. Kodaira, K. Osawa's Peculiar star HD221568. 1969, ApJ, Let., 157, 59

19. Schoneich, W., Hildebrandt, G., Furtig, W. Investigftion of the Light Variation of Twelve Ap Stars in Ten Spectral Regions. 1976, Astron. Nachr., 1, 297, 39

20. Schoneich, W. et al. Ten-colour Photometry of the Four Ap Stars HD 27309, HD 119213, HD170000, and HD 192913. 1976, Astron. Nachr., 4, 297, 173

21. Musielok, B. et al. Ten Colour Photometry of Twelve Ap-Stars. 1980, Astron. Nachr., 2, 301, 71

22. Preston, G.W. Surface characteristics of the magnetic stars. 1971, PASP, 83, 571

23. Musielok B. The Effect of Line Blocking on the Lightcurves of the Ap-Stars HD119213 HD170000 and HD173650. 1981, Acta Asnronomica, 31, 443

24. Molnar, M.R. Ultraviolet photometry forms the Orbiting Astronomical Observatory. VII. alpha 2 Canum Venaticorum. 1973, ApJ, L79, 527

25. Романюк, И.И. О некоторых проявлениях магнитного усиления линий поглощения в спектрах пекулярных звезд. 1984, Астрофизические Исследования, 18, 37

26. Maitzen, H.M. Ligh elektriseke Filterfotometric Fuld depression bei 5200 A in peculiar A-sternen, 1976, A&A, 51, 223

27. Kodaira, K. On the light Variation of Peculiar A-type Stars. 1973, A&A, 26, 385

28. Kupka, F.,Paunzen, E., Maitzen, H.M. The 5200-Åflux depression of chemically peculiar stars -I.Synthetic Δa photometry: The normality line. 2003,MNRAS, 341, 849

29. Tomley, L.J., Wallerstein, G., Wollf, S.C. A spectroscopic analysis of the silicon stars HD34452. 1974, A&A, 9, 380

30. Cowley, Ch.R. Element identifications in chemically peculiar stars of the upper main sequence. 1975, Physics of Ap-stars, IAU Colloquium, 32, 275

31. Kochukhov, O., Piskunov, N. Doppler Imaging of stellar magnetic fields. II. Numerical experiments, 2002, A&A, 388, 868

32. Страйжис, В., Житкявичюс, В. Выделение звезд Ap в Вильнюской фотометрической системе. 1977, Астрон. ж., 54, 5, 987

33. Илиев, И.Х. О едином механизме спектральной и фотометрической переменности пекулярных A звезд. 1983, Сообщения САО, 39, 3

34. Хохлова, В.Л. О возможной интерпретации переменности блеска и цвета магнитных Ap звезд с точки зрения модели наклонного ротатора. 1970, Астроном. ж., 48, 3, 534

35. Sokolov, N.A. Spectrophotometric Variability of the Magnetic CP Star alpha2 CVn. Magnetic Stars Proceedings of the International Conference, Nizhny Arkhyz, 2011, 390

36. Алышова, З.М., Алиев, С.Г., Халилов, В.М. Характер изменение блеска магнитных CP – звезд, Proceedings of the International Conference, Baku. 2018, 164

CP- MAQNİT ULDUZLARINDA FOTOMETRİK DƏYİŞKƏNLİYİN TƏDQİQİ 2. PARLAQLIĞIN DƏYİŞMƏSİ XÜSUSİYYƏTLƏRİ

Əliyev S.H, Xəlilov V.M., Alışova Z.M.

N.Tusi adına Şamaxı Astrofizika Rəsədxanası,
Azərbaycan Milli Elmlər Akademiyası, Şamaxı rayonu, Azərbaycan

Müxtəlif növ B0-F0 kimyəvi pekulyar maqnit ulduzlarının 10- rəngli fotometrik müşahidə materialları əsasında onların parlaqlığının faza əyriləri qurulmuşdur. Parlaqlıq əyrilərinin əksəriyyəti ikiqat dalğa kimi müşahidə olunur. Tədqiq olunan A2-F0 sinifinə mənsub SrCrEu tipli maqnit ulduzlarının parlaqlıqlarının müxtəlif zolaqlarda (filtrlərdə) əks faza ilə dəyişməsi müşahidə olunmuşdur.Göstərilmişdir, ki parlaqlığın əks faza ilə dəyimmısi miqdarı 4 - 6 dex çox olan nadir torpaq elementləri tərəfindən, spektrin $\lambda\lambda$5000 – 5500 ÅÅ oblastlarında (depressiya oblastında), enerjinin kəsilməz udulması vasitəsilə baş verir.

Açar sözlər: Maqnit ulduzları – Fotometrik dəyişkənliklər

1. CHRONICLE-2018

1. 1. On January 2, 2018, a scientific researcher of the department of Binary stars and eruptive processes, Gadzhiyev Musa Sadirovich, turned 80 years old (fired).

2. In ShAO, held an event dedicated to the memory of the victims January 20.

3. On January 30, 2018, the leading engineer of the Department of Information Communication Technologies and Organization, Seidov Abdul Aga Aziz Aga, turned 80 years old (fired).

4. January 31, 2018 held, the presentation of the book "Planets of the Solar System", of the head of the Department of Planets and Small Celestial Bodies of the Shamakhy Astrophysical Observatory, PhD in Physics Adalet Atai Abulfat.

5. On February 17, 2018, senior scientific researcher of the Department of Galaxies and star formation processes of the ShAO, Nadir Khanoglan Guliyev, turned 65 years old.

6. The Shamakhy Astrophysical Observatory named after N. Tusi hosted an event dedicated to March 1 - World Day of Civil Defense.

7. February 26, 2018, held an event dedicated to the Khojaly tragedy.

8. February 28, 2018, at the meeting of the Scientific Council, held elections for the post of head of scientific and scientific organizational structural units of the ShAO.

9. On March 2, 2018, in the frame of the project Reporting of the corporate and budgetary sector of the Ministry of Finance, private limited company SINAM, held a seminar on the use of “Financial and accounting reporting for budget organizations” together with the corresponding working group of the Ministry of Finance.

10. On March 24, 2018, the senior scientific researcher of the Department of Physics of Solar and Solar-Terrestrial Relations of the ShAO, Huseynov Shirin Shirinali turned 70 years old.

11. On March 25, 2018, the leading scientific researcher of the Department of Planets and Small Celestial Bodies of Shao, PhD in Physics and Mathematics, docent Zeinalov Rakhim Abutalib died.

12. From March 26 to March 30, 2018, the senior scientific researcher by the ShAO, Magerramov Yanus Mahmud, at the invitation of the Faculty of Natural Sciences, Department of Astronomy and Space Sciences, University of Istanbul, was on an academic trip in Istanbul, Republic of Turkey.

13. In connection with the Cosmonautics Day on April 12, by the Science Development under the President of the Republic of Azerbaijan and the Shamakhy Astrophysical Observatory named after N. Tusi, was organized an event for teachers and pupils of schools of the settlement named after Y. Mamedaliyev of Pirgulu and the village of Sabir of the Shamakhy district.

14. In connection with the Cosmonautics Day, on April 12, was organized an event by the Science Development Foundation under the President of the Republic of Azerbaijan, Tusi-Bohm Planetarium and the Shamakhy Astrophysical Observatory named after N. Tusi.

15. April 13 - the Vice-Rector for International Relations of Kharkov National University of Radio Electronics, Doctor of Technical Sciences, Professor Murad Anvar Omarov visited ShAO.

16. On April 14 Shamakhy Astrophysical Observatory. N. Tusi jointly with the Republican Center for the Development of Children and Youth of the Ministry of Education, Science Development Foundation under The President of the Republic of Azerbaijan, Knowledge Foundation under the President of the Republic of Azerbaijan, Planetarium Tusi Bohm held an event dedicated to the results of the "Show Me Space" competition.

17. On April 19, 2018, the Shamakhy Astrophysical Observatory held joint scientific discussions with the National Aviation Academy of Azerbaijan and Azercosmos.

18. On April 28-29, 2018, jointly with the Ministry of Taxes, The National Confederation of Entrepreneurs Organizations of the Republic of Azerbaijan, Chamber of Auditors, “Studying of Economic Resources” Public Union, the Azerbaijan Accountants and Risk Professionals Association (ARPA), Association of Professional Financial Managers (APFM), Center for Economic Research and Training, Young Accountants union, Azerbaijan Bank Training Center (ABTC) and the Azerbaijan University the 2nd National Forum of Accountants was organized at ShAO.

19. On March 14, 2018, by decision No. 7/23 of the Presidium of ANAS, Bagirli Sarkhan, Shabnam Agayeva and Zumrud Vidadi were admitted to the ShAO for doctoral studies for the preparation of a PhD.

20. On May 4, 2018, Professor Louis Ferrier, curator of meteorite collections at the Austrian Natural History Museum, presented a talk entitled "Meteorites and their impact craters on Earth what do we learn from them?"

21. On May 12,2018 Director of the Institute of Physics of the Earth named after Schmidt of the Russian Academy of Sciences, full member of RAS Roald Sagdeev, corresponding member of the RAS Sergey Tiksotsky, director of the laboratory of the Institute of Physics of the Earth named after Schmidt, Doctor of Physical and Mathematical Sciences Oleg Pokhotelov and academician-secretary of the department of Physical-Mathematical and Technical Sciences of ANAS Nazim Mamedov, held a scientific discussions in ShAO.

22. On May 31, 2018, the Trade Representative of the British Prime Minister Baroness Nicholson and the British Ambassador to Azerbaijan Carol Crofts visited the ShaO.

23. A regular scientific discussion on astrophysical experiments in nanosatellites, will be released in Azerbaijan for the first time, was held at the Shamakhy Astrophysical Observatory named after N.Tusi on June 5, 2018. Professor of the Department of Space Physics of Physics Faculty of the Moscow State University, S. Svertilov, Deputy Director for Science Research of the Institute of Nuclear Physics Scientific Research Institute named after D.V. Skobelchin, PhD in physics and mathematics V.Osedlo, senior scientific researcher of the institute, Y. Popova, Head of New Technology and Technology Development Department of the National Aviation Academy,A. Musayev and Head of Microelectronic Transmitters R. Ibrahimov participated at the meeting.

24. On June 7, the Science Development Foundation under President of Azerbaijan Republic announced the winners of the first Azerbaijani-Russian joint grant competition. Two grant projects from ShAO have won.

25. A scientific researcher at the Department of Space Plasma and Heliogeophysical Problems ShAO participated in the 24th conference of the International Planetary Society, held in Toulouse, France, from June 27 to July 5, 2018.

26. On June 29, 2018, summer cosmological camp "Asteroid Day", the largest camp in the field of cosmology and astronomy in Azerbaijan, was organized at ShAO.

27. On July 3-6, 2018, under the joint initiative of the Department of Chemical Sciences of ANAS and the Council of Young Scientists and Specialists of ANAS, was held an event called “Summer School of Young Chemists - 2018” for young people conducting an investigation in the field of chemistry.

28. The project presented by the head of the Department of Physics of Stellar Atmospheres and Magnetism of the Shamakhy Astrophysical Observatory named after N. Tusi, PhD in Phys. Mat. Sciences assistant professor Janmamed Rustamov is one of the winning projects of the largest grant project of the European Union "HORIZON-2020".

29. Two students entered the magistracy of ShAO.

30. Taking into account the large public interest in the Mars-Earth Opposition and the second Lunar eclipse in 2018, at Shamakhy Astrophysical Observatory named after N.Tusi and in Tusi-Bohm Planetarium from July 27 to July 28 to observe these events using telescopes were organized open days.

31. On July 28, 2018, Chief Specialist of the Public Relations Department of Shao, Nadir Khalilov turned 60 years old.

32. On August 10, 2018, a delegation led by the Ambassador Extraordinary and Plenipotentiary of the Republic of Korea to our country, Kim Chan-Kunun, visited the Shamakhy Astrophysical Observatory named after N. Tusi.

33. On 12-26 August 2018, a scientific researcher at the Department of galaxies and star formation processes of the Shao, Gunel Bahaddinova was on an academic trip at the Ondrejov Observatory of the Czech Republic.

34. On August 20-31, 2018, senior scientific researcher of the "Department of Planets and minor celestial bodies", of ShAO, PhD in astronomy Rustam Guliyev, took part in the General Assembly of the International Astronomical Union, (“XXX IAU General Assembly”) which held in Vienna, Austria.

35. On August 25, 2018, the first vice-president of Azerbaijan, the first lady of Azerbaijan, Mehriban Aliyeva, visited the 2-meter telescope of ShAO.

36. August 26 - September 1, 2018, junior scientific researcher of the Department "Space Plasma and Heliogeophysical Problems" of the Shao, Rajab Ismayilli took part in the International School of Young Astrophysicists of the CIS countries on the topic "Related problems of physics and astrophysics, high-energy particles" in city Alma-Ata of Kazakhstan Republic.

37. August 26 - September 1, 2018, scientific researcher of the Department of Space Plasma and Heliogeophysical Problems of ShAO, Mahir Pirguliev participated in the International School of Young Astrophysicists of the CIS countries on the topic "Related problems of physics and astrophysics, high-energy particles" in city Alma-Ata of Kazakhstan Republic.

38. The book of the head of the Department of Planets and minor celestial bodies of the Shamakhy Astrophysical Observatory named after N. Tusi, PhD in Physics, Associate Professor Adalet Atai, “Planets of the Solar System” was published (Publishing House "Lambert").

39. On September 3-7, 2018, junior scientific researcher of the Department of Space Plasma and Heliogeophysical Problems of the ShAO, Rajab Ismayıllı participated in the International School on the theme “BUKS 2018: Waves and instabilities in the solar atmosphere: Confronting the current state-of-the-art” organized in La Laguna, Tenerife, Spain.

40. September 17-21, 2018, Head of the Department of Binary stars and eruptive processes, PhD in Physical and Mathematical Sciences Bayram Rustamov participated in the International Conference "STARS-2018", which was held in St. Petersburg, Russian Federation.

41. September 17-21, 2018, Head of the Department of "Planets and minor celestial bodies", PhD in Physics, Associate Professor Adalet Atai participated in the International Conference "STARS-2018", which was held in St. Petersburg, Russian Federation.

42. Head of the Department of Galaxies and star formation processes of ShAO, Ismailov Nariman participated in the International Conference STARS-2018, held in St. Petersburg, Russian Federation from September 17 to September 21, 2018.

43. The head of the Department of Information Communication Technologies and Organization ShAO, Kamal Huseynov was on an academic trip at the Institute of Physics of the Earth named after Schmidt at the Russian Academy of Sciences from 10 to 20 September 2018, (Russian Federation, Moscow).

44. On September 26, 2018. The Chairman of the Bulgarian Academy of Sciences, Academician Julian Revalsky, Deputy Chairman of the Bulgarian Academy of Sciences, Corresponding Member Vasil Nikolov, Chief Scientific Secretary, Professor Evdokia Pasheva and Vice Mayor of Sofia, PhD in Archeology, Docent Todor Chobanov, visited ShAO.

45. The leading scientific researcher of the department of "Galaxies and star formation processes" of the Shao, PhD in Physics and Mathematics Sabir Aliyev, took part in the International conference on "Physics of Magnetic Stars", which held at the Special Astrophysics Observatory of the Russian Federation from 01 to 06 October 2018.

46. On October 3, 2018, was held a joint mobile meeting of the Presidium of ANAS and the Academic Council of Baku State University (BSU) at the Shamakhy Astrophysical Observatory named after N. Tusi of the National Academy of Sciences of Azerbaijan. Bakı A filial of the Department of Astrophysics of Baku State University and the centre of leisure for the effective spending of free time of the Academy staff in the observatory opened at the Shamakhy Astrophysical Observatory.

47. October 4-10, 2018, at the Shamakhy ShAO Astrophysical Observatory and Tusi-Bohm planetarium, open doors were held within the World Space Week.

48. On October 8-12, 2018, with joint organization of the Science Development Foundation under the President of the Republic of Azerbaijan, Shamakhy Astrophysical Observatory named after Nasraddin Tusi of ANAS, International Committee (ICG) on Global Navigation Satellite Systems (GNSS) under the United Nations Office on Outer Space Affairs (UNOOSA), the International Scientific Committee (ICS) on Solar-Earth Relations Physics (SCOSTEP), International “Space Weather Initiative” Program, Azercosmos OJSC and National Aviation Academy was held a international school-seminar on (The International Space Weather Initiative (ISWI) School on Space Weather (SW) and Global Navigation Satellite Systems) in Baku, Azerbaijan.

49. Shamakhy ShAO Astrophysical Observatory announced open day within the framework of "International Moon Observation Day" on October 20, 2018.

50. The Head of the Department of Physics of Stellar Atmospheres and Magnetism, of ShAO, Canmammad Rustamov was on an academic trip at the Moscow State University, the General Astronomical Institute (Russian Federation, Moscow) on November 5-11, 2018.

51. The senior scientific researcher of the Department of "Physics of Stellar Atmospheres and Magnetism" of ShAO, Khalilov Vagif Mahmud turned 70 years old on November 10, 2018.

52. Leading scientific researchers at the Shamakhy Astrophysical Observatory named after N. Tusi, D.I. Shestopalov and L.F. Golubeva published their books on "The composition of the matter of asteroids by their reflection spectra" ("Lambert" Publishing House).

53. On November 14, 2018, ShAO employees Mirnamik Bashirov, Mahir Pirguliev, Rajab Ismayilli spoke at the seminar on the presentation of some mathematical problems facing Astrophysics, for the employees of ANAS Institute of Mathematics.

54. On November 16-17, 2018, the International Conference "Physics and Lyrics: World Experience and the Realities of Science and Literature of the CIS Countries" was held.

55. From November 21 to November 28, 2018, Corresponding Member, of ANAS Director of ShAO, Namik Jalilov, was on an academic trip in the Russian Federation (Dubna, IZMIRAN).

56. Shamakhy Astrophysical Observatory named after N. Tusi of ANAS was awarded the prize in the nomination "The most productive regional university and scientific research institute" established by Web of Science Azerbaijan-2018.